Italian Journal of Geosciences
Bollettino della
Società Geologica Italiana
e del Servizio Geologico d'Italia

ISPRA
Istituto Superiore per la Protezione
e la Ricerca Ambientale
Dipartimento per il
SERVIZIO GEOLOGICO D'ITALIA
Organo Cartografico dello Stato (legge N°68 del 2.2.1960)

The fumarolic CO2 output from Pico do Fogo volcano (Cape Verde)

Journal:	*Italian Journal of Geosciences*
Manuscript ID	IJG-2020-0838.R1
Manuscript Type:	Original Article
Date Submitted by the Author:	n/a
Complete List of Authors:	Aiuppa, Alessandro; Università di Palermo Dipartimento di Scienze della Terra e del Mare, Bitetto, Marcello; Università di Palermo Dipartimento di Scienze della Terra e del Mare Rizzo, Andrea; Istituto Nazionale di Geofisica e Vulcanologia Sezione di Palermo Viveiros, Maria; Instituto de Investigação em Vulcanologia e Avaliação de Riscos Allard, Patrick; Institut de Physique du Globe de Paris Frezzotti, Maria Luce; Universita degli Studi di Milano-Bicocca Dipartimento di Scienze dell'Ambiente e del Territorio e di Scienze della Terra Valenti, Virginia; Università degli Studi di Milano-Bicocca Dipartimento di Scienze dell'Ambiente e del Territorio e di Scienze della Terra Zanon, Vittorio; Instituto de Investigação em Vulcanologia e Avaliação de Riscos
Keywords:	Pico do Fogo volcano, Cape Verde, volcanic gases, CO2 output

The fumarolic CO_2 output from Pico do Fogo volcano (Cape Verde)

Alessandro Aiuppa[1,*], Marcello Bitetto[1], Andrea L. Rizzo[2], Fatima Viveiros[3],
Patrick Allard[4], Maria Luce Frezzotti[5], Virginia Valenti[5], Vittorio Zanon[3,4]

[1]Dipartimento DiSTeM, Università di Palermo, Italy
[2]Istituto Nazionale di Geofisica e Vulcanologia, Sezione di Palermo, Italy
[3]Instituto de Investigação em Vulcanologia e Avaliação de Riscos, University of the Azores, Portugal
[4]Institute de Physique du Globe de Paris, Université de Paris, France
[5]Dipartimento di Scienze dell'Ambiente e della Terra, Università di Milano Bicocca, Italy
**Corresponding author: alessandro.aiuppa@unipa.it*

ABSTRACT

Pico do Fogo volcano, in the Cape Verde archipelago off the western coasts of Africa, has been the most active volcano in the Macaronesia region in the Central Atlantic, with at least 27 eruptions during the last 500 years. Between eruptions fumarolic activity has been persisting in its summit crater, but limited information exists for the chemistry and output of these gas emissions. Here, we use the results acquired during a field survey in February 2019 to quantify the quiescent summit fumaroles' volatile output for the first time. Combining measurements of the fumarole compositions (using both a portable Multi-GAS and direct sampling of the hottest fumarole) and of the SO_2 flux (using near-vent UV Camera recording), we quantify a daily output of 1060±340 tons CO_2, 780±320 tons H_2O, 6.2±2.4 tons H_2S, 1.4±0.4 tons SO_2 and 0.05±0.022 tons H_2. We show that the fumarolic CO_2 output from Pico do Fogo exceeds (i) the time-averaged CO_2 release during 2015-type recurrent eruptions and (ii) is larger than current diffuse soil degassing of CO_2 on Fogo Island. When compared to worldwide volcanoes in quiescent hydrothermal-stage, Pico do Fogo is found to rank among the strongest CO_2 emitters. Its substantial CO_2 discharge implies a continuous deep supply of magmatic gas from the volcano's plumbing system (verified by the low but measurable SO_2 flux), that becomes partially affected by water condensation and sulphur scrubbing in fumarolic conduits prior to gas exit. Variable removal of magmatic H_2O and S accounts for both spatial chemical heterogeneities in the fumarolic field and its CO_2-enriched mean composition, that we infer at 64.1±9.2 mol. % H_2O, 35.6±9.1 mol. % CO_2, 0.26±0.14 mol. % total Sulfur (S_t), and 0.04±0.02 mol. % H_2.

Keywords: *Pico do Fogo volcano; Cape Verde, volcanic gases, CO_2 output*

INTRODUCTION

Together with tectonic degassing, subaerial volcanism is the primary outgassing mechanism of mantle-derived CO_2 to the atmosphere (WERNER *et alii*, 2019; FISCHER *et alii*, 2019). Over geological time, tectonic and volcanic degassing have been the primary mechanisms for carbon exchange in and out our planet (DASGUPTA AND HIRSCHMANN, 2010; DASGUPTA, 2013; WONG *et alii*, 2019), ultimately playing a control role on pre-industrial atmospheric CO_2 levels and the climate (VAN DER MEER *et alii*, 2014; BRUNE *et alii*, 2017). Although attempts to estimate the global volcanic CO_2 output started early back in the 1990s (e.g., GERLACH, 1991), substantial budget refinements have only recently arisen from the 8-years (2011-2019) DECADE (Deep Earth Carbon Degassing; https://deepcarboncycle.org/about-decade) research program of the Deep Carbon Observatory (https://deepcarbon.net/project/decade#Overview) (FISCHER, 2013; FISCHER *et alii*, 2019).

One key result of DECADE-funded research has been the recognition that the global CO_2 output from subaerial volcanism is predominantly sourced from a relatively small number of strongly degassing volcanoes. AIUPPA *et alii*, (2019) showed that the top 91 SO_2 volcanic emitters in 2005-2015 (those systematically detected from space; CARN *et alii*, 2017) produce a cumulative CO_2

release of ~39 Tg/yr, nearly half of which (~19 Tg CO_2/yr) is produced by only 7 top-degassing volcanoes. It has also been found, however, that a non-trivial CO_2 output is additionally sustained by fumarolic degassing (FISCHER *et alii*, 2019; WERNER *at alii*., 2019) and groundwater transport (TARAN, 2009; TARAN AND KALACHEVA, 2019) at hydrothermal volcanoes in quiescent stage. These low-temperature (hydrothermal) fumarolic emissions typically release CO_2 in the absence of easily detectable (by Ultra Violet (UV) spectroscopy) SO_2, implying that traditional "indirect" CO_2 flux quantification using the volcanic gas CO_2/SO_2 ratio proxy in tandem with remotely sensed SO_2 fluxes (e.g. WERNER *et alii*, 2019) cannot be employed; more challenging airborne (WERNER *et alii*, 2009) or ground-based (PEDONE et alii, 2014; AIUPPA *et alii*, 2015; QUEIßER *et alii*, 2016) "direct" CO_2 flux measurements are required instead. These technical limitations have prevented us from establishing a robust catalogue for fumarolic CO_2 outputs, as <50 of the several hundred degassing volcanoes in "hydrothermal-stage" worldwide have been measured for their CO_2 flux (WERNER *et alii*, 2019). As a consequence, the extrapolated current inventories for the global fumarolic hydrothermal CO_2 flux (from 15 to 35 Tg CO_2/yr; FISCHER *et alii*, 2019; WERNER *et alii*, 2019) still involve very large uncertainties. In addition, most of the available information is for low-temperature arc volcanic gases, while much less is known for the fumarolic CO_2 output for non-arc settings (divergent, intra-plate or continental rift; e.g., ILYINSKAYA *et alii*, 2015, 2018).

Pico do Fogo, in the Cape Verde archipelago, makes part of the Macaronesia region, an area of the Atlantic Ocean off the western coasts of Africa also including the archipelagos of the Azores, Madeira and Canary (Fig. 1). This 2829 m a.s.l high strato-volcano (Fig. 2a), located on the island of Fogo, has been the most frequently erupting volcanic centre of the Macaronesia region in the last 500 years (RIBEIRO, 1960). All historical eruptions occurred on its upper flanks or in its summit crater. Between eruptions, the summit crater of Pico do Fogo hosts a persistent fumarolic field (Fig. 2b-e), with several gas vents ranging in temperature from boiling to >200°C (DIONIS *et alii*, 2014; MELIÁN *et alii*, 2015). The CO_2 output sustained by diffuse degassing across the crater floor was estimated in the range 147±35 (in 2009) to 219±36 t/d (in 2010) (DIONIS *et alii*, 2014, 2015), but no comparable data yet exists for the fumarolic CO_2 output itself.

Here we fill this gap of knowledge by presenting the very first results for the fumarolic output of CO_2 and other volatiles from Pico do Fogo. These results were obtained from a gas survey on February 5, 2019, during which we combined real-time in-situ measurement of the crater gas compositions (Multi-GAS), direct sampling of the hottest fumarole, and near-vent remote sensing of the SO_2 flux with an UV Camera. Our new data set contributes to improved quantification and understanding of Fogo's quiescent degassing during the multi-decadal phases separating eruptions, and offers an interesting comparison with the gas output measured during the recent 2014-2015 eruption (HERNÁNDEZ et alii, 2015). More broadly, our results for Pico do Fogo add a novel piece of information to the still fragmentary data base for fumarolic CO_2 emissions from global volcanoes in hydrothermal stage.

FOGO ISLAND AND PICO DO FOGO VOLCANO

The Cape Verde archipelago, extending between 15 and 17°N latitude 500 km to the west of Senegal, is composed of 10 main islands that are the emerged portions of a high oceanic plateau (2 km above the sea floor). Fogo Island is located at the south-western edge of this system (Fig. 1). The Cape Verde oceanic Rise, the world's largest geoid and bathymetric seafloor anomaly (COURTNEY & WHITE, 1986), has been interpreted as due to a hot-spot mantle swell centred north-east of the Sal island (CROUGH, 1978, 1982; HOLM *et alii*, 2008). The presence of an active mantle plume beneath the northern part of Cape Verde at least has been suggested by some authors based on seismic imaging (MONTELLI *et alii*, 2006; LIU & ZHAO, 2014; SAKI *et alii*, 2015). A mantle plume contribution is also consistent with high primordial ^3He ($^3He/^4He$ ratios up to 12.3-15.7 Ra) in volcanics from Sao Vicente and Sao Nicolau islands (CHRISTENSEN *et alii*, 2001; DOUCELANCE *et alii*, 2003; MATA *et alii*, 2010; MOURÃO *et alii*, 2012). However, a plume origin for Macaronesian volcanism is still matter of debate (Bonatti, 1990; Asimov *et alii*, 2004), and the role of decompressional melting (Métrich *et alii*, 2014) favoured by extensional lithospheric discontinuities (Marques *et alii*, 2013) has received increased attention recently. Volcanism on the Cape Verde Islands is thought to have started 24–22 Ma ago on the northeastern islands, followed by a more recent westward migration of volcanic activity (both in the northern and southern branches of the archipelago) during the Pliocene-Pleistocene (Holm *et alii*, 2008). Erupted products spread a large compositional range but mafic, silica-undersaturated lavas (basanites, tephrites, and nephelinites) prevail (Gerlach *et alii*, 1988; Davies *et alii*, 1989; Holm *et alii*, 2006), eventually associated with rarer carbonatites (Kogarko *et alii*, 1992; Hoernle *et alii*, 2002). Trace-element and isotope geochemistry of the erupted volcanics are extremely heterogeneous, with significant differences between the northern and southern islands, implying the probable involvement of several distinct mantle sources: a lower mantle plume containing both mixed HIMU (High $\mu = {}^{238}$□/^{204}□□ at zero age) and EM1 (Enriched Mantle 1) end-members, possibly a 1.6-Ga recycled oceanic crust, plus the depleted upper mantle (northern islands) and the subcontinental lithospheric mantle (southern islands) (Gerlach *et alii*, 1988; Davies *et alii*, 1989; Holm *et alii*, 2006; Christensen *et alii*, 2001; Doucelance *et alii*, 2003; Millet *et alii*, 2008). The actual relative proportions of each of these sources are still debated however.

Fogo Island (Fig. 1b), formed during the last 3-4.5 Ma, has been the single site of historical volcanic activity (27 reported eruptions) since the discovery of the Cape Verde archipelago in the XV^th^ century. The dominant structure of the island is Monte Amarelo volcano~~,~~ whose summit was truncated by three massive flank collapses between ca. 60 and 43 ka (Fig. 1b) (Day *et alii*, 1999; 2000; Marques *et alii*, 2020). The post-collapse (62 ka to present) activity has been primarily concentrated within the Chã das Caldeiras depression (Fig. 1b), leading to progressive infilling of the collapse scar and the formation of the Pico do Fogo cone. The cone itself (Fig. 2a) has remained the primary eruptive centre until 1785 (Ribeiro, 1960), when fissure-fed effusive eruptions became concentrated along the flanks of Pico, occurring at an average frequency of one every ~50 years. The most recent eruptions happened in 1951 (HILDNER *et alii*, 2012), 1995 (HILDNER *et alii*, 2011) and 2014-2015 (CARRACEDO *et alii*, 2015; CAPPELLO *et alii*, 2016; RICHTER *et alii*, 2016; MATA *et alii*, 2017). Eruptive products of the Amarelo-Fogo volcanic complex are primarily alkali-rich tephritic to basanitic lavas (with rarer foidites and more evolved phonolites). They are thought to ascend from a 16–28 km deep magma storage zone, emplaced in the underlying lithospheric mantle (GERLACH *et alii*, 1988; DOUCELANCE *et alii*, 2003; HILDNER *et alii*, 2011, 2012; MATA *et alii*, 2017).

MATERIALS AND METHODS

On February 5, 2019 we realized extensive field investigations and measurements of the summit crater fumarolic emissions of Pico de Fogo volcano (Fig. 2a-e). We used a portable Multi-component Gas Analyser System (Multi-GAS) to analyse in real-time the fumaroles' compositions during walking traverses across the fumarolic field (see the track shown in Figure 2e). The walking traverse mode, first used on Vulcano Island (AIUPPA *et alii*, 2005a), is ideal to explore the chemical heterogeneity of a fumarolic field as a high number of fumarolic vents can sequentially be analysed while slowly moving along the path. During the traverse, the Multi-GAS continuously acquired data at 0.5 Hz, and its position was synchronously geo-localized with an embedded GPS. In addition to areas of diffuse soil degassing, 17 main fumarolic vents, showing the strongest emissions, were identified during the traverse (Fig. 2e). Gas composition at each of these vents was determined (Tab. 1) by keeping the MultiGAS inlet at a constant position (and for a few minutes) at about ~50 cm height above the fumarolic vent. Our Multi-GAS instrument comprised the following sensor combination (e.g., AIUPPA *et alii*, 2016): a Gascard EDI030105NG infra-red spectrometer for CO_2 (Edinburgh Instruments; range: 0-30,000 ppmv); 3 electrochemical sensors for SO_2 (T3ST/F-TD2G-1A), H_2S (T3H-TC4E-1A) and H_2 (T3HYT- TE1G-1A), all from City Technology; and a

KVM3/5 Galltec-Mela temperature (T) and relative humidity (Rh) sensor. H_2O concentration in the fumarolic gases was calculated from co-acquired T, Rh and pressure readings using the Arden Buck equation (see AIUPPA *et alii*, 2016). Reading from the H_2S sensor were corrected for 14% cross-sensitivity to SO_2. Gas ratios in each of the main fumaroles (Tab. 1) were derived from scatter plots of the gas concentrations using the Ratiocalc software (TAMBURELLO, 2015). Uncertainties in all derived ratios are <15%, except for H_2O/H_2S ($\leq 25\%$).

The fumarole 15, displaying the highest emission temperature ($T = 315°C$), was sampled for dry gases only by inserting a titanium tube 50 cm-long into the vent. This tube was connected to both a quartz line equipped with a condenser in order to remove water vapour and a three-way valve with a syringe allowing to force gas flow into the line. Three dry gas samples were stored in glass bottles equipped of two stopcocks and then moved to the INGV laboratory in Palermo for chemical analysis. Concentrations of He, H_2, O_2, N_2, CO, CH_4, CO_2 and H_2S were determined using a gas chromatograph (Clarus 500, Perkin Elmer) equipped with a 3.5-m column (Carboxen 1000) and a double detector (hot-wire detector and flame ionization detector [FID]). SO_2 was not measurable with this sampling/analytical setup. Analytical errors were <3%. The results are reported in Tab. 2.

Simultaneously to our Multi-GAS traverse, we also operated a portable dual UV camera system for measuring the volcanic SO_2 flux. The camera system registered at 0.5 Hz for ~100 minutes from a fixed position on the inner crater terrace's rim, deep inside the summit crater (see Figs. 2b, 2e). The system used two co-aligned cameras (JAI CM-140GE-UV), both fitted with optical lenses of 45° Field of View, and mounting two different band-pass optical filters with Full Width at Half Maximum (FWHM) of 10 nm and central wavelengths of 310 and 330 nm, respectively. The filters were applied in front of the cameras so to achieve differential UV absorption in the SO_2 band (KANTZAS *et alii,* 2009; KERN *et alii*, 2010; DELLE DONNE *et alii*, 2019). The system, housed in a peli case and powered by a 12V LiPo battery, was mounted on a tripod and rotated to look upward to image the crater's inner northern slope (where the fumarolic field is located) and a portion of the background sky (Figs. 2b, 2d). Data acquisition was commanded via PC using the Vulcamera software (TAMBURELLO *et alii* 2011). The acquired images (520x676 pixels at 10-bit resolution) were post-processed using standard techniques (KANTZAS *et alii*, 2009; TAMBURELLO *et alii*, 2011, 2012): sets of co-acquired images were combined into absorbance images and were then converted into SO_2 slant column amount (SCA) images by successively using three different calibration cells. Finally, we derived an Integrated Column Amount (ICA) time-series by integrating the SCA along the cross-section shown in Fig. 2b and then the SO_2 flux by multiplying the ICA with the plume speed. The plume speed (1.9±0.6 m/s) was obtained by processing image sequences acquired at 0.2 Hz using a LifeCam Cinema HD (Microsoft) USB visible camera, integrated in the UV Camera system. Processing involved quantifying the rising speeds of ~50 individual gas puffs of well-resolved structure, moving upward from the fumarolic field toward the crater edge (Fig. 2d).

Finally, from the same position as the UV camera, we used a portable handheld thermal camera (model FLIR E5) in order to acquire a thermal map of the fumarolic field (see Fig. 2b). This map allowed us to verify that the hottest degassing areas were in large part covered by the Multi-GAS traverse. Temperatures of fumaroles 5 and 14-15, the hottest vents in the field (Fig. 2b), were also directly measured in situ with a portable thermocouple.

RESULTS

FUMAROLIC GAS COMPOSITION: MULTI-GAS AND DIRECT SAMPLING

As a whole, during the ~74-minute duration of our Multi-GAS traverse we obtained 4446 simultaneous measurements of H_2O, CO_2, SO_2, H_2S and H_2 concentrations in Fogo gas emissions (one analysis every 2 seconds). The entire dataset is illustrated in Figure 3 where the gas concentrations in the near-vent fumarolic plumes are displayed as scatter plots. The concentrations of H_2O, CO_2 and H_2 were corrected for the respective air background values of ~12,000, ~600 and ~0.5 ppmv measured upwind (outside) the fumarolic field (Fig. 2e). The high background CO_2

concentration compared to "normal" atmosphere (~400 ppmv) is explained by the high diffuse soil CO_2 emission through the inner crater floor (DIONIS *et alii*, 2014, 2015).

The absolute gas concentrations measured along our traverse display quite large variations (Fig. 3), indicating chemical heterogeneity in the fumarolic field emissions. This is especially evident in the SO_2 vs. H_2S scatter plot (Fig. 3). Otherwise, one observes broad co-variations among most gas species, even though with some spread. The maximum peak values reached ~23,000 (H_2O), ~20,000 (CO_2), 118 (H_2S), 62 (SO_2) and 30 (H_2) ppmv.

The molar compositions of fumarolic gases from the 17 individualized vents (Tab. 1) confirm this spatial heterogeneity. Each fumarole actually exhibited stable, well-resolved composition (see the fumarole 15 example in Figure 3). Instead, the SO_2/H_2S ratios in all fumaroles span more than three orders of magnitude, from 0.001 to 1.5 (Tab. 1 and Fig. 3). The H_2O/H_2S, CO_2/H_2S, and H_2/H_2S also varied considerably within the fumarolic field, with respective ranges of 98-480, 108-240 and 0.05-0.24 (Tab. 1 and Fig. 3).

Table 2 shows the chemistry of dry gases collected from the hottest (315°C) F15 fumarole (Fig. 2d, e). CO_2 is the overwhelming component (up to 97%), followed by H_2S (around 1%), H_2 (952-979 ppm), CO (15-17 ppm) and CH_4 (around 1-2 ppm). N_2 and O_2 contents reflect air contamination of the samples, with minimum values of 0.5% and 0.1%. The concentration of helium is around 8 ppm in our less contaminated sample. Whatever the degree of air contamination, our samples from the hottest F15 fumarole reveal CO_2/H_2S (94-107) and H_2/H_2S (0.09-0.10) ratios (Tab. 2) that are very comparable to the corresponding ratios determined with Multi-GAS.

The SO_2/H_2S ratio is a commonly used marker to distinguish the magmatic (SO_2-rich) vs. hydrothermal (H_2S-rich) nature of volcanic gas (e.g. AIUPPA *et alii*, 2005b). Figure 4 shows that Pico do Fogo fumaroles define a nearly continuous trend from two end-members:

(i) a magmatic end-member, represented by the hottest gas from fumaroles 14-15 (T = 315-316 °C), characterized by H_2O/CO_2 of ~ 2, CO_2/S_t of ~ 100, high SO_2 (~0.2 mol. %) and relatively low H_2S, and oxidised (redox conditions of about 1 log unit above the Nickel-Nickel Oxide buffer at ~500°C, estimated from the measured SO_2/H_2S ~ 0.9-1.4 and H_2/H_2O ~ 0.0004; see methodology in AIUPPA et al., 2011); and,

(ii) a hydrothermal end-member, represented by fumaroles 3-8, that is H_2S-dominated (~0.35-0.43 mol. %; SO_2/H_2S of ~ 0.01-0.2), relatively richer in CO_2 (CO_2/S_t > 130 and H_2O/CO_2 < 1) and more reduced (H_2/H_2O > 0.0015) (corresponding to redox conditions close to the FeO-FeO1.5 buffer; GIGGENBACH, 1987).

The red star in Figures 4a-d represents the spatially integrated composition of Pico do Fogo's fumarolic emission, calculated as the arithmetic mean of compositions of the 17 main fumaroles. It is characterized by the following ratios, normalized to H_2S: SO_2/H_2S = 0.3±0.4, H_2O/H_2S = 299±109, CO_2/H_2S = 153±33 and H_2/H_2S = 0.2±0.04 (Tab. 1). The mean SO_2/H_2S ratio of ~0.3 is not much different from the SO_2/H_2S ratio of 0.12 of the bulk volcanic plume (Tab. 1 and Fig. 4) determined after 30-min continuous Multi-GAS measurements made on the outer crater rim (see "bulk plume Multi-GAS site" in Fig. 2b, e). At that Multi-GAS site, we could intercept only a very dilute plume, rising buoyantly from the fumarolic field inside the crater floor (Fig. 2d). Only small concentrations of H_2S (~ 1 ppmv) and SO_2 (~ 0.15 ppmv) could be detected, no volcanic H_2O, CO_2, or H_2 being resolvable from the air background. Given these very low H_2S and SO_2 concentrations, well below our calibration range (10-200 ppmv), the inferred bulk plume SO_2/H_2S ratio of 0.12 must be considered with caution; we just take it as indication that hydrothermal H_2S-rich fumaroles prevail over the more magmatic end-member fumaroles in the bulk gas emission from Pico do Fogo, in agreement with indications from the arithmetic mean of fumarolic compositions.

SO_2 FLUX

Figure 5a presents the SO_2 flux time-series obtained by the UV Camera on February 5, 2019. A plot of SO_2 column amounts along the UV cross-section of Fig. 5b shows that, thanks to the short distance (~200 m) between the camera and the targeted plume, a feeble but continuous SO_2 emission (<400 ppm·m; mean, 140±110 ppm·m) was detected by the UV Camera in the leftmost portion of the camera FoV (Fig. 5c), and persisted throughout the ~100 minutes of recording (Fig. 5a). During our measurement interval the SO_2 flux varied between 0.3 and 2.3 tons/day (or 0.009 to 0.06 kg/s) and averaged at 1.4±0.4 tons/day (0.016±0.004 kg/s).

DISCUSSION

THE COMPOSITION OF PICO DO FOGO FUMAROLES

The molar gas ratios determined by Multi-GAS measurements allow us to compute the molar percentages of H_2O, CO_2, H_2S, SO_2 and H_2 in each fumarole and in the mean gas composition (Table 1). These percentages for only the 5 above species are upper bounds since we did not determine other possible minor species (N_2, HCl) in the gases. Otherwise, they are not affected by the presence of reduced carbon species, whose amount was verified to be very low in F5 fumarole this study and (MELIÁN *et alii*, 2015). According to our results, the Pico do Fogo fumaroles are moderately hydrous (41-73 % H_2O; mean, 64 %), CO_2-rich (27-59 %; mean, 36 %), and contain about ~0.3 % S_t and 0.04 % H_2 (Tab. 1). These mean values match well the composition of the F15 fumarole, directly sampled and analysed in laboratory, as regards the H_2/H_2S and CO_2/H_2S molar ratios (Tab. 2).

The triangular plot in Figure 6 puts the H_2O-CO_2-S_t compositions of our Pico do Fogo fumaroles in a wider context, by comparing them against the compositions of (i) the 2014 Fogo eruption plume (HERNÁNDEZ *et alii*, 2015), which represents the only available datum for the Fogo magmatic gas signature to date; (ii) magmatic gases from other intraplate, rift and/or divergent-plate volcanoes (see AIUPPA, 2015 for data sources); and (iii) fumaroles from other volcanic systems in the Macaronesia region, including the Azores (CALIRO *et alii*, 2005; FERREIRA & OSKARSSON, 1999; FERREIRA *et alii*, 2005; MARES project, this study) and Teide in the Canary (MELIÁN *et alii*, 2012; MARES project, this study).

The Pico do Fogo summit fumaroles (this study) are compositionally distinct from the magmatic gases released during the 2014 eruption (HERNÁNDEZ *et alii*, 2015), this latter falling well within the range of measured magmatic gas compositions at other intraplate volcanoes (yellow field, from AIUPPA, 2015). More specifically, the summit Fogo fumaroles are evidently S-depleted relative to the 2014 magmatic gas, which strongly suggests intense sub-surface scrubbing of reactive S compounds under the "hydrothermal" conditions of the fumarolic field, where surface temperatures (≤ 315 °C) are well below the boiling temperature of liquid sulfur (455 °C; above which S scrubbing become minimal, if any; AIUPPA *et alii*, 2017). Extensive S deposition in the sub-surface environment of the summit fumaroles is further supported by CO_2/S_t ratios being far higher in the fumaroles (93-162) than in the 2014 eruption gas (1.5; HERNÁNDEZ *et alii*, 2015) (Figs. 6, 7). The two hottest summit fumaroles (F14 and F15) consistently display the lowest CO_2/S_t ratios (93-97), but these are still two orders of magnitude higher than in the eruptive gas, confirming the importance of sulfur scrubbing (Fig. 7). This is also verified for the dry gases directly sampled from fumarole F15, whose CO_2/H_2S ratio is 94-107 (Tab. 2).

Fogo summit fumaroles are also less hydrous (or more CO_2-rich) than the 2014 eruptive gas (Fig. 6). If the 2014 gas is representative of the magmatic gas feeding the summit fumaroles (a magmatic gas supply is indeed supported by the low but measurable SO_2 output; Fig. 5), then the simplest explanation of H_2O depletion in the fumaroles is extensive steam condensation in the fumarolic conduits due to low temperature conditions. Because our Multi-GAS measurements were made in air-diluted (and cooled) fumarolic plumes, we cannot entirely exclude that partial H_2O condensation could have also occurred during plume transport and/or in the Multi-GAS inlet system (tubing + filter), such as previously observed at other volcano-hydrothermal systems (e.g., ALLARD *et alii*, 2014; LOPEZ *et alii,* 2017; TAMBURELLO *et alii*, 2019). However, we note that our Multi-GAS-derived H_2O range (41-73 %) partially overlaps with the H_2O range (52-92 %) for the summit Fogo fumaroles previously determined from direct gas sampling (MELIÁN *et alii*, 2015). We thus conclude that both subsurface and within-plume H_2O condensation may combine to drive the summit fumaroles toward a less hydrous and correspondingly CO_2-enriched composition compared to the 2014 eruptive gas. We cannot exclude, however, that the magmatic gas that feeds the persistent summit fumaroles is compositionally different from the 2014 eruptive gas. If for example the magmatic gas source is the Pico do Fogo magma reservoir located in the uppermost mantle at 16–28 km depth (HILDNER et alii, 2011, 2012; MATA et alii, 2017), then it is well possible that its composition has deeper (CO_2-richer, H_2O-S-poorer) signature than that of eruptive 2014 gas (derived from shallow degassing).

The Pico do Fogo fumaroles plot at the CO_2-rich end of the compositional array defined by volcanic hydrothermal fluids in the Macaronesian region (Fig. 6). The majority of volcanic fumaroles from the Azores (Sao Miguel, Terceira and Graciosa islands) and from Teide volcano in the Canaries are shifted toward the H_2O corner. This is a typical (but not exclusive) feature of most hydrothermal steam vents worldwide (CHIODINI & MARINI, 1998), which reflects their derivation from the boiling of meteoric groundwater-fed hydrothermal systems (CALIRO *et alii*, 2015). The less hydrous compositions of Pico do Fogo fumaroles suggest the absence of a shallow boiling hydrothermal aquifer underneath Pico's summit, and consequently a weaker (relative to Azores and Teide) hydrothermal fingerprint (greater magmatic signature), especially in the hottest fumaroles (F14 and F15) that also exhibit lower CO_2/S_t ratios (Fig. 7) and higher SO_2/H_2S ratios (Fig. 4). These SO_2-bearing F14-F15 fluids appear as formerly magmatic gases that have undergone partial H_2O-S_t loss (via condensation + scrubbing) during cooling and hydrothermal re-equilibration (Fig. 6). Instead, the most SO_2-poor, H_2S-dominated fumaroles (e.g., F3-F8) have suffered more significant hydrothermal processing, as testified by their lower H_2O/CO_2 (< 1), higher CO_2/S_t (> 130), and more reduced (H_2-rich) redox conditions, typical of hydrothermal fluids (FISCHER & CHIODINI, 2015) (Figs. 4, 7).

To conclude, we attribute the CO_2-rich compositions of the Pico do Fogo fumaroles to a combination of (i) hydrothermal interactions (partially removing magmatic sulphur and water) and possibly (ii) a deep magmatic gas source.

GAS OUTPUT BUDGET

Combining the compositional data described above with the UV camera-based SO_2 flux record depicted in Figure 5, we can reliably estimate the output of CO_2 and other volatiles from the summit crater fumarolic field of Pico do Fogo (Table 3). To do this calculation, we combine the measured mean SO_2 flux (1.4±0.4 tons/day) and the mean molar composition of the summit fumaroles (64.1±9.2 % H_2O, 35.6±9.1 % CO_2, 0.2±0.08 % H_2S, 0.06±0.06 % SO_2, and 0.04±0.02 % H_2; red star in Figs. 4, 6 and 7), the S_t (0.26±0.14 %) of which is scaled to the bulk plume SO_2/H_2S ratio of 0.12 (Tab. 1 and Fig. 4) to infer the bulk plume mass ratios at 558 (H_2O/SO_2), 756 (CO_2/SO_2), 4.2 (H_2S/SO_2) and 1.1 (H_2/SO_2), respectively. This procedure allows us to smooth the effect of the large compositional heterogeneity of the fumarolic vents. We just note that the bulk plume SO_2/H_2S ratio of 0.12 characterizes the predominance of H_2S-dominated (F3-F8-like) hydrothermal fluids over more SO_2-rich (F14-F15-like) "more magmatic" fumaroles.

We obtain a daily fumarolic CO_2 output of 1060±340 tons (Table 3). We also estimate a daily release of 780±320 H_2O, 6.2±2.4 H_2S and 0.05±0.022 H_2. These results demonstrate that the fumarolic gas output is larger, for all volatiles, than diffuse degassing through the crater floor (DIONIS *et alii*, 2014, 2015) (Fig. 8). For example, the latter has been estimated to produce 147-219 (±35) tons/day of CO_2 (DIONIS *et alii*, 2014, 2015), which is only 14-20% of the inferred fumarolic CO_2 output. Even considering the soil CO_2 output estimated at the scale of the entire island (828±5 tons/day; DIONIS *et alii*, 2015), the contribution of diffuse degassing remains less than a half (~ 43%) of the total Fogo island CO_2 degassing budget (~1890 tons/day; this study and DIONIS *et alii*, 2015).

In contrast, the daily fumarolic gas output is far lower than the eruptive gas output (Fig. 8) for the 2014 eruption derived by HERNÁNDEZ *et alii*, (2015) by combining SO_2 flux measurements with a scanning UV spectrometer (using the Differential Optical Absorption Spectroscopy – DOAS - technique) and a Multi-GAS-derived plume composition. Our fumarolic SO_2 output, for example, is a factor ~7000 lower than the large (~10 ktons) daily eruptive release (HERNÁNDEZ *et alii*, 2015). Let emphasize, however, that while summit fumarolic emissions at Fogo have persisted as a stable degassing feature over the past few centuries (RIBEIRO, 1960), eruptive degassing has been restricted to the relatively infrequent eruptions. There are only 10 reported eruptions since 1785 (RIBEIRO, 1960), of which only 3 since 1951 (HILDNER *et alii*, 2011, 2012; CARRACEDO *et alii*, 2015; MATA *et alii*, 2017). Between June 12, 1951 (the onset of the first, well recorded XX century eruption; HILDNER *et alii*, 2012) and February 8, 2015 (the end of the last eruption), Fogo has been in eruption for only 200 days (e.g., 0.008 % of the 24710 elapsed days). If we take the November 30, 2015 gas output (HERNÁNDEZ *et alii*, 2015) as typical for Fogo eruptive daily degassing rate, we can roughly compute a cumulative eruptive release for 1951-2015 (200 days of eruption) of ~4 Mtons of H_2O, ~2 Mtons of CO_2 and SO_2, 11 ktons of H_2S and 0.04 ktons of H_2. These masses, when scaled to (integrated over) the 24710 days elapsed from June 12, 1951 to February 8, 2015, correspond to daily eruptive outputs of only 196, 86, 82, 0.5 and 0.002 tons/day for H_2O, CO_2, SO_2, H_2S and H_2, respectively (Fig. 8). Our back-of-the-envelop calculations demonstrate that, when examined on longer-term perspective, eruptive emissions at Fogo are significant for only SO_2, while they do make a relatively small contribution to the emission budget of other volatiles (Fig. 8).

We therefore conclude that summit crater fumarolic emissions at Pico do Fogo are the dominant source of volcanic CO_2 (and most other volatiles) over multi-decadal scale.

IMPLICATIONS FOR THE GLOBAL CO_2 OUTPUT INVENTORY

On a broader perspective, our results for Pico do Fogo in Cape Verde archipelago add a new piece of information to the global catalogue of volcanic CO_2 emissions. Recent work (FISCHER *et alii*, 2019; WERNER *et alii*, 2019) has attempted at refining the global volcanic CO_2 emission inventory, by reviewing, cataloguing and synthesizing the volcanic CO_2 output information available in the international literature. It was found that, by late 2019, CO_2 flux measurements have become available for 102 of the ~500 degassing subaerial volcanoes worldwide (FISCHER *et alii*, 2019; WERNER *et alii*, 2019; FISCHER & AIUPPA, 2020 submitted). Different strategies have been used to extrapolate the cumulative CO_2 output "measured" for the 102 volcanoes (~44 Tg/yr) to CO_2 emissions from the several hundred "unmeasured" subaerial degassing volcanoes. These have included the use of independent rock-chemistry information (AIUPPA *et alii*, 2019) and/or the identification of statistical properties (mean CO_2 output and confidence intervals) for different categories of volcanoes. On the latter basis, it was proposed that the present-day global volcanic CO_2 budget is dominated by the category of Strong Volcanic Gas Emitters (S_{vge}) – which includes the ~100 top degassing volcanoes whose SO_2 emissions are systematically detected from space-borne and/or ground-based spectrometers (CARN *et alii*, 2017; FISCHER *et alii*, 2019). S_{vge} have an inferred total (extrapolated) CO_2 output of ~ 36-39 Tg/yr (AIUPPA *et alii*, 2019; FISCHER *et alii*, 2019). It was additionally found that a group of Weak Volcanic Gas Emitters (W_{vge}), although degassing in a more subtle manner (this category includes volcanoes with no visible plumes and/or minor to absent SO_2 emissions), may still contribute between 15 (FISCHER et alii, 2019) and 35 (WERNER *et alii*, 2019) Tg CO_2/yr, simply because they are numerous (~400) globally. Unfortunately, however, these results are subject to very large uncertainties because measuring the CO_2 output from quiescent/hydrothermal volcanoes is especially challenging from a technical viewpoint (indirect SO_2 flux-based estimates are hampered by low to absent SO_2; WERNER *et alii*, 2019), making the CO_2 flux catalogue particularly incomplete for W_{vge}.

Pico do Fogo falls within the W_{vge} category, as no plume is visually observable (Fig. 2) and no SO_2 is detectable by satellite except during the infrequent eruptions (GLOBAL VOLCANISM PROGRAM, 2017). Our results show, however, that SO_2 is present in tiny but measurable quantities in the fumaroles (Table 1), making both the SO_2 flux and, indirectly, the CO_2 flux (Table 3) measurable from a very proximal location on ground (Fig. 2; note that a test made with UV-Camera from the base of the volcano were unable to detect any SO_2 release).

When put in the context of global volcanic CO_2 fluxes (Fig. 9; data from FISCHER *et alii*, 2019), the fumarolic CO_2 flux from Pico do Fogo (ca. 1000 tons/day) confirms that W_{vge} volcanoes can emit CO_2 in quantities that, in some cases, can rival the emissions of S_{vge} volcanoes. High CO_2 emission from such W_{vge} systems, despite negligible (hydrothermal-dominant) to weak (magmatic-hydrothermal) SO_2 emission (FISCHER *et alii*, 2019), result from their exceptionally high CO_2/S_t signature (AIUPPA *et alii*, 2017). Pico do Fogo fumaroles are not an exception, but owing to their high CO_2/S_t compositions they can sustain a CO_2 output of order 1000 tons/day, at the upper range of the global W_{vge} and S_{vge} populations (Fig. 9). Therefore, our present results further demonstrate that refining the global inventory for volcanic CO_2 output will require enhanced quantification of the weaker, poorly visible emissions sustained by quiescent hydrothermal volcanoes, the majority of which still lack CO_2 flux quantification.

CONCLUSIONS

We have shown here that fumarolic activity on-top of Pico do Fogo volcano, in the Atlantic Cape Verde archipelago, is currently a poorly visible but substantial source of volcanic volatiles to the atmosphere. The fumarolic CO_2 output (~1060 tons/day), in particular, is found to exceed by far the time-integrated eruptive CO_2 flux (~86 tons/day) from the volcano, as well as the estimated total CO_2 budget from soil degassing across Fogo island (147-828 tons/day). On a broader scale, our results confirm that quiescent volcanoes characterized by hydrothermal activity during quiescent stages can produce CO_2 emissions that rival those of more manifestly degassing (Strong Volcanic Gas Emitters, S_{vge}) owing to their CO_2-enriched fumarole compositions (CO_2/S_t ratios of 93-163 at Pico do Fogo in 2019). At Pico do Fogo, these CO_2-enriched compositions likely result from the interactions (scrubbing of magmatic sulphur, and water condensation) of a deep magmatic gas supply (perhaps sourced from a 16–28 km deep magma reservoir in the uppermost mantle; HILDNER *et alii*, 2011, 2012; MATA *et alii*, 2017) with a shallow hydrothermal system.

ACKNOWLEDGEMENTS

This research was funded by the Portuguese Fundacão para a Ciência e a Tecnologia (MARES project - PTDC/GEO-FIQ/1088/2014), the DECADE project of the Deep Carbon Observatory, and the Italian Ministero Istruzione Università e Ricerca (Grant n. 2017LMNLAW). We thank Francesco Salerno and Manfredi Longo from INGV-Palermo for providing support with gas chromatographic analysis. The manuscript benefited from constructive reviews from Taryn Lopez, Yuri Taran and from the Associate Editor Orlando Vaselli.

REFERENCES

AIUPPA A. (2015) - *Volcanic-gas monitoring* In: *Volcanism and Global Environmental Change*, pp. 81-96. Cambridge University Press. doi: 10.1007/9781107415683.007.

AIUPPA A., FEDERICO C., GIUDICE G. & GURRIERI S. (2005a) - *Chemical mapping of a fumarolic field: La Fossa Crater, Vulcano Island (Aeolian Islands, Italy)*. Geophysical Research Letters, **32**, 4.

AIUPPA A., INGUAGGIATO S., MCGONIGLE A.J.S., O'DWYER M., OPPENHEIMER C., PADGETT M.J., ROUWET D. & VALENZA M. (2005b) - *H_2S fluxes from Mt. Etna, Stromboli, and Vulcano (Italy)* *and implications for the sulfur budget at volcanoes*. Geochim. Cosmochim. Acta, **69 (7)**, 1861-1871.

AIUPPA A., SHINOHARA H., TAMBURELLO G., GIUDICE G., LIUZZO M., MORETTI R., (2011) – *Hydrogen in the gas plume of an open-vent volcano, Mount Etna, Italy*. J. Geophys. Res. B: Solid Earth **116** (10), B10204.

AIUPPA A. ET ALII (2015) - *New ground-based lidar enables volcanic CO_2 flux measurements*. Sci. Reports **5**, 13614.

AIUPPA A., LO COCO E., LIUZZO M., GIUDICE G., GIUFFRIDA G. & MORETTI R. (2016) - *Terminal Strombolian activity at Etna's central craters during summer 2012: The most CO2-rich volcanic gas ever recorded at Mount Etna*. Geochemical Journal, **50 (2)**, 123-138.

AIUPPA A., FISCHER T.P., PLANK T., ROBIDOUX P. & DI NAPOLI R. (2017) - *Along-arc, interarc and arc-to-arc variations in volcanic gas CO_2/S_T ratios reveal dual source of carbon in arc volcanism*. Earth Science Reviews **168**, 24–47.

AIUPPA A., FISCHER T.P., PLANK T. & BANI P. (2019) - *CO_2 flux emissions from the Earth's most actively degassing volcanoes, 2005–2015*. Sci. Reports **9**:5442, https://doi.org/10.1038/s41598-019-41901-y.

ALLARD P., AIUPPA A., BEAUDICEL, GAUDIN D., DI NAPOLI R., CRISPI O., CALABRESE S., PARELLO F., HAMMOUYA G., TAMBURELLO G. (2014) *Steam and gas emission rate from La Soufriere volcano, Guadeloupe (Lesser Antilles): implications for the magmatic supply during degassing unrest*. Chemical Geology **384**, 76–93

ASIMOW P.D., DIXON J.E. & LANGMUIR C.H. (2004) - A *hydrous melting and fractionation model for mid-ocean ridge basalts: application to the Mid-Atlantic Ridge near the Azores*. Geochemistry, Geophysics, Geosystems **5**, doi:10.1029/2003GC000568.

BONATTI E. (1990) - *Not so hot 'hot spots' in the oceanic mantle.* Science **250**, 107-111.

BRUNE S., WILLIAMS S.E. & MÜLLER R.D. (2017) - *Potential links between continental rifting, CO_2 degassing and climate change through time*. Nat. Geosci., **10**, 941–946. doi: 10.1038/s41561-017-0003-6.

CALIRO S., VIVEIROS F., CHIODINI G. & FERREIRA T. (2015) - *Gas geochemistry of hydrothermal fluids of the S. Miguel and Terceira Islands, Azores*. Geochimica et Cosmochimica Acta, **168**, 43-57. doi: 10.1016/j.gca.2015.07.009.

CAPPELLO A., GANCI G., CALVARI S., PÉREZ N.M., HERNÁNDEZ P.A., SILVA S.V., CABRAL J. & DEL NEGRO C. (2016) - *Lava flow hazard modeling during the 2014-2015 Fogo eruption, Cape Verde*. Journal of Geophysical Research: Solid Earth, **121 (4)**, pp. 2290-2303.

CARN S.A., FIOLETOV V.E., MCLINDEN C.A., LI C. & KROTKOV N.A. (2017) - *A decade of global volcanic SO_2 emissions measured from space*. Sci. Reports **7**:44095, doi: 10.1038/srep44095.

CARRACEDO J.-C., PEREZ-TORRADO F.J., RODRIGUEZ-GONZALEZ A., PARIS R., TROLL V.R. & BARKER A.K. (2015) - *Volcanic and structural evolution of Pico do Fogo, Cape Verde*. Geology Today, **31 (4),** pp. 146-152.

CHIODINI G. & MARINI L. (1998) - *Hydrothermal gas equilibria: The H_2O-H_2-CO_2-CO-CH_4 system*. Geochim. Cosmochim. Acta, **62 (15)**, 2673-2687. doi: 10.1016/S0016-7037(98)00181-1.

CHRISTENSEN B., HOLM P., JAMBON A. & WILSON J. (2001) - *Helium, argon and lead isotopic composition of volcanics from Santo Antão and Fogo, Cape Verde Islands*. Chemical Geology, **178**, 127–142.

COURTNEY R.C. & WHITE R.S. (1986) - *Anomalous heat-flow and geoid across the Cape- Verde rise — evidence for dynamic support from a thermal plume in the mantle*. Geophysical Journal International, **87** (3), 815–867.

CROUGH S.T. (1978) - *Thermal origin of mid-plate hot-spot swells*. Geophys. J. R. Astron. Soc., **55**, 451– 469.

CROUGH S.T. (1982) - *Geoid anomalies over the Cape Verde Rise*. Mar. Geophys. Res., **5**, 263–271, doi:10.1007/BF00305564.

DASGUPTA R. (2013). *Ingassing, storage, and outgassing of terrestrial carbon through geologic time*. Rev. Mineral. Geochem., **75**, 183–229. doi: 10.2138/rmg.2013.75.7.

DASGUPTA R. & HIRSCHMANN M.M. (2010) - *The deep carbon cycle and melting in Earth's interior*. Earth Planet. Sci. Lett., **298**, 1–13. doi: 10.1016/j.epsl.2010.06.039.

DAVIES G.F., NORRY M.J., GERLACH D.C. & CLIFF R.A. (1989) - *A combined chemical and Pb-Sr-Nd isotope study of the Azores and Cape Verde hotspots: The geodynamic implications, in Magmatism in the Ocean Basins*. In Saunders A.D. & Norry M.J. Geol. Soc. Spec. Publ., **42**,231–255.

Day, S.J., Heleno Da Silva, S.I.N., Fonseca, J.F.B.D. A past giant lateral collapse and present-day flank instability of Fogo, Cape Verde Islands (1999) Journal of Volcanology and Geothermal Research, 94 (1-4), pp. 191-218.

Day, S.J., Carracedo, J., Guillou, H., Pais Pais, F., Rodriguez Badiola, E., Fonseca, J., Heleno da Silva, S., 2000. Comparison and cross-checking of historical, archaeological and geological evidence for the location and type of historical and sub-historical eruptions of multiple-vent oceanic island volcanoes. In: McGuire, W., Griffiths, D., Hancock,P., Stewart, I. (Eds.), The Archaeology of Geological Catastrophes: Geological Society, London, Special Publications, London, pp. 281–306.

DELLE DONNE D., AIUPPA A., BITETTO M., D'ALEO R., COLTELLI M., COPPOLA D., PECORA E., RIPEPE M. & TAMBURELLO G. (2019) - *Changes in SO_2 Flux regime at Mt. Etna captured by automatically processed ultraviolet camera data.* Remote Sensing, **11 (10)**, art. no. 1201.

DIONIS S.M., MELIÁN G., RODRÍGUEZ F., HERNÁNDEZ P.A., PADRÓN E., PÉREZ N.M., BARRANCOS J., PADILLA G., SUMINO H., FERNANDES P., BANDOMO Z., SILVA S., PEREIRA J.M. & SEMEDO H.

(2014) - *Diffuse volcanic gas emission and thermal energy release from the summit crater of Pico do Fogo, Cape Verde*. Bulletin of Volcanology, **77** (2), 13 p.

Dionis S.M., Pérez N.M., Hernández P.A., Melián G., Rodríguez F., Padrón E., Sumino H., Barrrancos J., Padilla G.D., Fernandes P., Bandomo Z., Silva S., Pereira J.M., Semedo, H. & Cabral J. (2015) - *Diffuse CO_2 degassing and volcanic activity at Cape Verde Islands, West Africa*. Earth, Planets and Space, **67 (1)**, art. no. 48.

Doucelance R., Escrig S., Moreira M., Gariepy C. & Kurz M.D. (2003) - *Pb-Sr-He isotope and trace element geochemistry of the Cape Verde Archipelago*. Geochim. Cosmochim. Acta, **67**, 3717–3733.

Ferreira T. & Oskarsson N. (1999) - *Chemistry and isotopic composition of fumarole discharges of Furnas caldera*. J. Volcanol. Geotherm. Res. **92**, 169–179.

Ferreira T., Gaspar J.L., Viveiros F., Marcos M., Faria C. & Sousa F. (2005) - *Monitoring of fumarole discharge and CO_2 soil degassing in the Azores: contribution to volcanic surveillance and public health risk assessment*. Ann. Geophys. **48**, 787–796.

Fischer T.P. (2013) - *DEep CArbon DEgassing: The Deep Carbon Observatory DECADE Initiative*. Mineralogical Magazine, **77(5)**, 1089.

Fischer T.P. & Aiuppa A. (2020). *Global CO_2 emissions from subaerial volcanism: recent progresses and future challenges*. Geochem. Geophys., Geosyst., under consideration.

Fischer T.P. & Chiodini G. (2015). *Volcanic, Magmatic and Hydrothermal Gases*. In: The Encyclopedia of Volcanoes, 2nd Edition, Edited by H. Sigurdsson, B. Houghton, S. McNutt, H. Rymer, J. Stix Elsevier, doi: 10.1016/B978-0-12-385938-9.00045-6

Fischer T.P., et alii (2019) - *The emissions of CO_2 and other volatiles from the world's subaerial volcanoes*. Sci. Rep., **9**:18716, https://doi.org/10.1038/s41598-019-54682-1.

GERLACH D.C., CLIFF C.A., DAVIES G.R., NORRY M.J. & HODGSON N. (1988) - *Magma sources of the Cape Verdes archipelago: Isotopic and trace element constraints*. Geochim. Cosmochim. Acta, **52**, 2979–2992. doi:10.1016/0016-7037(88)90162-7.

GERLACH T.M. (1991) - *Present-day carbon dioxide emissions from volcanoes*. Earth in Space 4, 5.

Global Volcanism Program, 2017. Report on Fogo (Cape Verde). In: Crafford A.E. & Venzke E. (eds.), Bulletin of the Global Volcanism Network, **42**, 9. Smithsonian Institution. https://doi.org/10.5479/si.GVP.BGVN201709-384010.

GIGGENBACH W.F. (1987), *Redox processes governing the chemistry of fumarolic gas discharges from White Island, New Zealand*, Appl. Geochem., **2**, 143–161, doi:10.1016/0883-2927(87)90030-8.

HERNÁNDEZ P.A. (2015) - *Chemical composition of volcanic gases emitted during the 2014-15 Fogo eruption, Cape Verde*. Geophysical Research Abstracts, Vol. **17**, EGU2015-9577, 2015, EGU General Assembly 2015.

HILDNER E., KLÜGEL A. & HAUFF F. (2011) - *Magma storage and ascent during the 1995 eruption of Fogo, Cape Verde Archipelago*. Contributions to Mineralogy and Petrology, **162 (4)**, 751. doi:10.1007/s00410-011-0623-6.

HILDNER H., KLÜGEL A. & HANSTEEN T. (2012) - *Barometry of lavas from 1951 eruption of Fogo, Cape Verde Islands: implications for historic and prehistoric magma plumbing system*. Journal of Volcanology and Geothermal Research, **217**-218, 73–90.

HOERNLE K., TILTON G., LE BAS M.J., DUGGEN S. & GARBE-SCHÖNBERG D. (2002) - *Geochemistry of oceanic carbonatites compared with continental carbonatites: mantle recycling of oceanic crustal carbonate*. Contributions to Mineralogy and Petrology, **142(5)**, 520-542.

HOLM P.M., WILSON J.R., CHRISTENSEN B.P., HANSEN L., HANSEN S.L., HEIN K.M., MORTENSEN A.K., PEDERSEN R., PLESNER S. & RUNGE M.K. (2006) - *Sampling the Cape Verde mantle plume:*

evolution of the melt compositions on Santo Antão, Cape Verde Islands. Journal of Petrology, **47**, 145–189.

Holm P.M., Grandvuinet T., Friis J., Wilson J.R., Barker A.K. & Plesner S. (2008) - *An ^{40}Ar–^{39}Ar study of the Cape Verde hot spot: temporal evolution in a semistationary plate environment*. Journal of Geophysical Research **113 (B8)**, B08201.

Kantzas E.P., McGonigle A.J.S., Tamburello G., Aiuppa A. & Bryant R.G. (2010) - *Protocols for UV camera volcanic SO_2 measurements*. J. Volcanol. Geothem. Res., **194**, 55–60.

Kern C., Kick F., Lübcke P., Vogel L., Wöhrbach M. & and Platt U. (2010) - *Theoretical description of functionality, applications, and limitations of SO_2 cameras for the remote sensing of volcanic plumes*. Atmos. Meas. Tech., **3**, 733–749, www.atmos-meas-tech.net/3/733/2010/ doi:10.5194/amt-3-733-2010.

Kogarko L.N., Ryabukhin V.A. & Volynets M.P. (1992), *Cape Verde Island carbonatite geochemistry*. Geochem. Int., **29**, 62–74.

Ilyinskaya E, Aiuppa A, Bergsson B et alii (2015) - *Degassing regime of Hekla volcano 2012-2013*. Geochim. Cosmochim. Acta, **159**. 80-99.

Ilyinskaya E., Mobbs S., Burton R., Burton M., Pardini F., Pfeffer M.A., et alii (2018) - *Globally significant CO_2 emissions from Katla, a Subglacial Volcano in Iceland*. Geophys. Res. Lett., **45**, 332–310. doi: 10.1029/2018GL079096.

Liu X. & Zhao D. (2014) - *Seismic evidence for a mantle plume beneath the Cape Verde hotspot*. International Geology Review, **56**, 1213–1225.

Lopez T., et alii, (2017) - *Geochemical constraints on volatile sources and subsurface conditions at Mount Martin, Mount Mageik, and Trident Volcanoes, Katmai*. J. Volcanol. Geotherm. Res., **347** 64–81, https://doi.org/10.1016/j.jvolgeores.2017.09.001.

MARQUES F.O., CATALÃO J.C., DEMETS C., COSTA A.C.G. & HILDENBRAND A. (2013) - *GPS and tectonic evidence for a diffuse plate boundary at the Azores Triple Junction*. Earth and Planetary Science Letters **381**, 177-187.

MARQUES F.O., HILDENBRAND A., VICTÓRIA S.S., CUNHA D. & DIAS, P. (2020) - *Caldera or flank collapse in the Fogo volcano? What age? Consequences for risk assessment in volcanic islands*. Journal of Volcanology and Geothermal Research (in press), https://doi.org/10.1016/j.jvolgeores.2019.106686

MATA J., MOREIRA M., DOUCELANCE R., ADER M. & SILVA, L.C. (2010) - *Noble gas and carbon isotopic signatures of Cape Verde oceanic carbonatites: implications for carbon provenance*. Earth and planetary Science Letters, **291**, 70–83.

MATA J., MARTINS S., MATTIELLI N., MADEIRA J., FARIA B., RAMALHO R.S., SILVA P., MOREIRA M., CALDEIRA R., RODRIGUES J. & MARTINS L. (2017) - *The 2014–15 eruption and the short-term geochemical evolution of the Fogo volcano (Cape Verde): Evidence for small-scale mantle heterogeneity*. Lithos, **288–289**, 91–107.

MELIÁN G., TASSI F., PÉREZ N., HERNÁNDEZ P., SORTINO F., VASELLI O., PADRÓN E., NOLASCO D., BARRANCOS J., PADILLA G., RODRÍGUEZ F., DIONIS S., CALVO D., NOTSU K. & SUMINO H. (2012) - *A magmatic source for fumaroles and diffuse degassing from the summit crater of Teide Volcano (Tenerife, Canary Islands): A geochemical evidence for the 2004-2005 seismic-volcanic crisis*. Bulletin of Volcanology, **74 (6)**, 1465-1483.

MELIÁN G.V., ET ALII (2015) - *Insights from fumarole gas geochemistry on the recent volcanic unrest of Pico do Fogo, Cape Verde*. Geophysical Research Abstracts, Vol. **17**, EGU2015-12754, 2015, EGU General Assembly 2015.

MÉTRICH N., ZANON V., CRÉON L., HILDENBRAND A., MOREIRA M., MARQUES F.O. (2014) - *Is the "Azores hotspot" a wet spot? Insights from geochemistry of fluid and melt inclusions in olivines of Pico basalts*. J. Petrol. **55**, 377-393

MILLET M.A., DOUCELANCE R., SCHIANO P., DAVID K. & BOSQ C. (2008) - *Mantle plume heterogeneity versus shallow-level interactions: a case study, the São Nicolau Island, Cape Verde archipelago*. Journal of Volcanology and Geothermal Research, **176(2)**, 265-276.

MONTELLI R., NOLET G., DAHLEN F.A. & MASTERS G. (2006) - *A catalogue of deep mantle plumes: new results from finite-frequency tomography*. Geochemistry, Geophysics, Geosystems **7**, http://dx.doi.org/10.1029/2006GC001248

MOURÃO, C., MOREIRA, M., MATA, J., RAQUIN, A., MADEIRA, J (2012) *Primary and secondary processes constraining the noble gas isotopic signatures of carbonatites and silicate rocks from Brava Island: evidence for a lower mantle origin of the Cape Verde plume*. Contributions to Mineralogy and Petrology **163**, 995–1009.

PEDONE M. ET ALII (2014) - *Volcanic CO_2 flux measurement at Campi Flegrei by tunable diode laser absorption spectroscopy*. Bulletin of Volcanology, **76**, 13.

QUEIßER M., GRANIERI D. & BURTON M. (2016) - *A new frontier in CO_2 flux measurements using a highly portable DIAL laser system*. Scientific Reports, **6**, 33834.

RIBEIRO O. (1960) - *A Ilha do Fogo e as suas erupcões (The island of Fogo and its eruptions)*. 2nd edn. Memorias, serie geographica I. Junta de Investigacões do Ultramar. Ministerio do Ultramar, Lisbon.

RICHTER N., FAVALLI M., DE ZEEUW-VAN DALFSEN E., FORNACIAI A., DA SILVA FERNANDES R.M., PÉREZ N.M., LEVY J., VICTÓRIA S.S. & WALTER T.R. (2016) - *Lava flow hazard at Fogo Volcano, Cabo Verde, before and after the 2014-2015 eruption*. Natural Hazards and Earth System Sciences, **16 (8)**, pp. 1925-1951.

Saki, M., Thomas, C., Nippress, S.E.J., Lessing, S., 2015.Topography of upper mantle seismic discontinuities beneath the North Atlantic: the Azores, Canary and Cape Verde plumes. Earth and Planetary Science Letters 409, 193–202

TAMBURELLO G. (2015) - *Ratiocalc: Software for processing data from multicomponent volcanic gas analyzers*. Comput. Geosci., **82**, 63–67.

TAMBURELLO G., KANTZAS E.P., MCGONIGLE A.J.S. & AIUPPA A. (2011) - *Vulcamera, a program for measuring volcanic SO_2 using UV cameras*. Ann. Geophys. **54**, 2.

TAMBURELLO G., AIUPPA A., KANTZAS E.P., MCGONIGLE A.J.S. & RIPEPE M. (2012) - *Passive vs. active degassing modes at an open-vent volcano (Stromboli, Italy).* Earth Planet. Sci. Lett., **359–360**, 106–116.

TAMBURELLO G., MOUNE S., ALLARD P., VENUGOPAL S., ROBERT V., ROSAS-CARNAJAL M., UCCIANI G., DEROUSSI S, KITOU T., DIDIER T., KOMOROWSKI J-C., BEAUDICEL F., DE CHABALIER J-B., LEMARCAHND A., MORETTI R., DESSERT C. (2019) *Spatio-temporal relationships between fumarolic activity, hydrothermal fluid circulation and geophysical signals at an arc volcano in degassing unrest: La Soufrière of Guadeloupe (French West Indies).* Geosciences, **9**, 480-507 doi:10.3390/geosciences9110480.

TARAN, Y., KALACHEVA, E. (2019) - *Role of hydrothermal flux in the volatile budget of a subduction zone: Kuril arc, northwest Pacific*. Geology, 47 (1), 87-90. doi: 10.1130/G45559.1

TARAN, Y.A. (2009) - Geochemistry of volcanic and hydrothermal fluids and volatile budget of the Kamchatka-Kuril subduction zone Geochimica et Cosmochimica Acta, 73 (4), 1067-1094. , doi: 10.1016/j.gca.2008.11.020

VAN DER MEER D.G., ZEEBE R.E., VAN HINSBERGEN D.J.J., SLUIJS A., SPAKMAN W. & TORSVIK T.H. (2014) - *Plate tectonic controls on atmospheric CO_2 levels since the Triassic*. Proc. Natl. Acad. Sci. U.S.A. 111, 4380–4385. doi:10.1073/pnas.1315657111.

WERNER C., EVANS W. C., POLAND M., TUCKER D.S. & DOUKAS M.P. (2009) - *Long-term changes in quiescent degassing at Mount Baker Volcano, Washington, USA; evidence for a stalled intrusion in 1975 and connection to a deep magma source*. Journal of Volcanology and Geothermal Research **186**, 379–386.

WERNER C., ET ALII, (2019) - *Carbon Dioxide Emissions from Subaerial Volcanic Regions: Two Decades in Review*. In: Orcutt B.N, Daniel I. & Dasgupta R. *Deep Carbon, Past to Present*. Cambridge University Press www.cambridge.org/9781108477499, doi: 10.1017/9781108677950.

WONG K, MASON E., BRUNE S, EAST M., EDMONDS M. & ZAHIROVIC S. (2019) - *Deep Carbon Cycling Over the Past 200 Million Years: A Review of Fluxes in Different Tectonic Settings*. Front. Earth Sci. **7**, 263. doi: 10.3389/feart.2019.00263.

FIGURE CAPTIONS

Figure 1 - Google Earth image (Image © 2019 Maxar Technologies) of (a) the Cape Verde archipelago and (b) Fogo Island.

Figure 2 – (a) Panoramic view of Pico do Fogo volcano; (b) Map of the Pico do Fogo summit crater, showing (i) a thermal map of the fumarolic field; (ii) the position of the 17 analysed fumaroles (red circles, see (e) for a detail; white numbers identify fumaroles 1, 8 and 17 for reference); (iii) the UV Camera measurement site (FOV and "cross section" are the Field of View of the camera and the ICA integration section, respectively); and (iv) the Bulk-plume Multi-Gas measurement site. The base map is from Bing Maps (https://www.bing.com/maps, Microsoft Ltd); (c) the inner crater seen from the Bulk-plume Multi-Gas measurement site; (d) the fumarolic field seen from the UV Camera measurement site. The plume transport direction is indicated by white arrows. The position of some selected fumaroles (red circles with identification numbers) are shown for reference; (e) A zoom of the inner crater (base map as in (a)), showing the track of the Multi-GAS walking traverse and the positions of the 17 fumaroles (red circles with white labels; see Tab 1 for GPS positions). All measurements were performed on February 5, 2019.

Figure 3 – Scatter plots of H_2O, CO_2, SO_2 and H_2 concentrations vs H_2S in the plumes of summit crater fumaroles at Pico do Fogo. Open circles stand for the 4446 concentration

measurements performed during the ~74-minute-long Multi-GAS walking traverse. H_2O, CO_2 and H_2 concentrations are corrected for air background (see text). In each plot, solid lines and grey-filled area identify the range (minimum, maximum) of X/H_2S gas ratios in the identified 17 individual fumaroles (see Table 1). The large spread of compositions, indicated by the large ratio interval (especially for the SO_2/H_2S ratio, varying from 0.001 to 1.5), attests to the chemical heterogeneity of the fumarolic field. Otherwise, each of the 17 fumaroles exhibited stable, well-resolved X/H_2S ratios, as here illustrated by the F15 fumarole example (grey-filled circles).

Figure 4 – Scatter plots of SO_2/H_2S ratios in the 17 fumaroles vs. (a) H_2O/H_2S ratios, (b) H_2O/CO_2 ratios, (c) CO_2/S_t ratios, and (d) H_2/H_2O ratios (data from Table 1). The SO_2/H_2S ratio is taken as a good indicator of the magmatic (high-SO_2) vs. hydrothermal (high-H_2S) signature of each fumarole. The measured fumaroles define a nearly continuous trend between a “magmatic” gas end-member, represented by the SO_2-richer, hydrous ($H_2O/CO_2 \sim 2$) and more oxidised (low H_2/H_2O) F14-F15 fumaroles, and a hydrothermal (H_2S-dominated) end-member (exemplified by fumaroles F3-F8), richer in CO_2 ($CO_2/S_t > 130$ and $H_2O/CO_2 < 1$) and more reduced ($H_2/H_2O > 0.0015$). Note that we directly collected 3 dry-gas samples of fumarole F15 for comparison, which yield a CO_2/S_t ratio range of 94-107 (Table 2; pink horizontal bar labelled “DS” in (c)) nearly identical to the Multi-GAS-derived ratio (97; Table 1). In each plot the red star identifies the average (arithmetic mean of the 17 fumaroles) composition of the fumarolic field (Table 1), while the vertical grey bar (“BULK”) indicates the SO_2/H_2S ratio measured in the bulk plume from the outer rim (site in Fig. 2).

Figure 5 – (a) SO_2 flux time-series obtained with the UV Camera from the “UV Camera” measuring site indicated in Figure 2. Blue diamonds are individual data (obtained every 2 seconds) while the red line is for a 60 sec mobile average; (b) a pseudo-colour image obtained by combination of two simultaneously taken (by the two co-exposed UV cameras) images, showing the inner crater wall, and the ICA integration section (UV cross-section); (c) an example of SO_2 column

amount (in ppm·m) variation along the camera pixels over the UV cross-section shown in (b). The plume is identified by higher-than-background SO_2 column amounts (0-400 ppm·m) between camera pixels 0 and ~200.

Figure 6 – $H_2O/10$-CO_2-$5S_t$ triangular plot comparing the compositions of Pico do Fogo summit fumaroles (yellow circles, data from Table 1; red star mean composition as in Figure 4) with the compositions of (i) the 2014-2015 Fogo eruptive plume (orange circle labelled "FO"; HERNÁNDEZ *et alii*, 2015) (ii) hydrothermal vents from the Macaronesia (see legend) and worldwide (crosses; CHIODINI & MARINI, 1998). Also shown for comparison are the compositional fields of arc magmatic gases and intraplate/rift magmatic gases (AIUPPA, 2015). The white circles identify compositions for some intraplate /rift volcanoes (HE: Hekla; ER: Erebus; NY: Nyiragongo; KI: Kilauea summit; KE: Kilauea east rift zone; AR: Ardoukoba; PDF: Piton de la Fournaise; EA: Erta Ale; SU: Surtsey; see AIUPPA, 2015 for data provenance). Grey lines identify some characteristic CO_2/S_t and H_2O/CO_2 ratios (see grey numbers on axes). The effects of S scrubbing, H_2O condensation or addition are illustrated by the red lines (with arrows).

Figure 7 – (a) Temperature dependence of CO_2/S_t (molar) ratios in the Macaronesia fumarolic gas samples. At Pico do Fogo, we measured temperatures (with a thermocouple) in only the three hottest vents (F5, F14 and F15). The CO_2/S_t (molar) ratios in hydrothermal fluids from volcanoes in the Azores and from Teide (Tenerife, Canary) are shown for comparison in both (a) and in the zoom of (b). The latter shows that CO_2/S_t ratios in fumaroles from Azores-Canary are negatively correlated with temperature, as observed globally (AIUPPA *et alii*, 2017). For reference, we also show in both panels the CO_2/S_t ratio signature of Fogo magmatic gas, as determined by Multi-GAS plume measurements during the 2014-2015 eruption (HERNÁNDEZ *et alii*, 2015; see also Figure 6).

Figure 8 – Volatile outputs from different types of gas emissions on Fogo island: (i) the summit fumarolic field, this study; (ii) diffuse soil degassing from the crater area and the whole island

(DIONIS et alii, 2014, 2015); and (iii) eruptive degassing (HERNÁNDEZ *et alii*, 2015 and recalculated; see text for explanation).

Figure 9 – Histogram showing the logarithmic distribution of the population of measured/predicted CO_2 fluxes (in tons/day) from subaerial volcanoes. Data are from Fischer et alii, (2019) except for Pico do Fogo (this study). Following FISCHER *et alii*, (2019) and FISCHER & AIUPPA (2019, submitted), volcanoes are distinguished in two sub-categories: 1) Strong Volcanic Gas Emitters (S_{vge}, in red), including the 125 top degassing volcanoes whose SO_2 emissions have systematically been detected from space-borne and/or ground-based spectrometers (CARN *et alii*, 2017; FISCHER *et alii*, 2019); and 2) Weak Volcanic Gas Emitters (W_{vge}), including volcanoes with no visible plumes and weak SO_2 emissions. Like in FISCHER et alii, (2019) and FISCHER & AIUPPA, (2020, submitted), W_{vge} are further divided into hydrothermal volcanoes, with minor to absent (< 8 tons/day) SO_2 emissions (yellow), and magmatic-hydrothermal volcanoes with somewhat higher (> 8 tons/day, but still undetectable from space) SO_2 emissions (orange). Pico do Fogo, although falling in the subcategory of W_{vge} (SO_2 < 8 tons/day) emits CO_2 at the upper W_{vge} range, and at levels comparable to (or higher than) many S_{vge}.

Table 1 – Results of Multi-GAS observations on Pico do Fogo fumarolic field on February 5, 2019. We report composition obtained for 17 fumaroles, the atmospheric plumes of which were measured for a few minutes each (time start – time end is GMT time). Temperature was measured in three fumaroles only using a portable thermocouple. For each fumarole, we report the peak SO_2 concentration (SO_2 max) measured during the acquisition interval and the volatile ratios (normalised to H_2S) calculated with Ratiocalc (Tamburello, 2015) using the scatter-plot technique. For each ratio, mean is the slope of the best-fit regression line and R^2 is the corresponding correlation coefficient. We also report the recalculated molar percentages (mol. %) in the fumaroles and some representative molar ratios. *Mean fumarole composition (and 1 standard deviation, 1 SD) calculated by averaging the compositions of the 17 fumaroles. The bulk plume was measured for its SO_2/H_2S ratio only from the crater rim site shown in Figure 2. £Ratios determined on the same F15 fumarole using direct sampling (data from Tab. 2).

Fumarole ID	**T**	**LAT**	**LONG**	**Time Start**	**Time End**	**SO_2 max**	**Mean**	**R^2**	**Error**	**Mean**	**R^2**	**Error**	**Mean**	**R^2**	**Error**	**Mean**	**R^2**	**Error**	**mol%**	**mol%**	**mol%**	**mol%**	**mol%**	**molar**	**molar**	**molar**	**molar**
	°C					**ppm**	**SO_2/H_2S**	**SO_2/H_2S**	**SO_2/H_2S**	**CO_2/H_2S**	**CO_2/H_2S**	**CO_2/H_2S**	**H_2/H_2S**	**H_2/H_2S**	**H_2/H_2S**	**H_2O/H_2S**	**H_2O/H_2S**	**H_2O/H_2S**	**H_2O**	**CO_2**	**H_2S**	**SO_2**	**H_2**	**H_2O/CO_2**	**H_2O/S_{tot}**	**CO_2/S_t**	**H_2/H_2O**
1		14.95046	-24.34111	13:27	13:30	3.9	0.15	0.85	0.04	149	0.99	10	0.18	0.884	0.04	318	0.97	39	67.9	31.8	0.21	0.03	0.04	2.1	276	130	0.00057
2		14.95063	-24.34071	13:31	13:32	4.9	0.16	0.65	0.12	136	0.96	30	0.13	0.848	0.06	260	0.97	49	65.5	34.2	0.25	0.04	0.03	1.9	224	117	0.00050
3		14.95069	-24.34072	13:32	13:33	0.6	0.001	0.53	0.01	135	0.99	37	0.165	0.99	0.03	98	0.94	55	41.7	57.8	0.43	0.00	0.07	0.7	98	135	0.00169
4		14.9507	-24.34072	13:33	13:36	3.8	0.05	0.53	0.03	117	0.94	20	0.13	0.677	0.06	184	0.90	59	61.0	38.6	0.33	0.02	0.04	1.6	175	111	0.00071
5	225	14.95067	-24.3408	13:36	13:40	8.8	0.14	0.65	0.06	133	0.99	8	0.15	0.91	0.03	284	0.96	33	68.0	31.7	0.24	0.03	0.04	2.1	249	116	0.00053
6		14.95066	-24.34072	13:41	13:46	5.2	0.36	0.90	0.22	134	0.99	7	0.18	0.918	0.03	277	0.96	27	67.2	32.4	0.24	0.09	0.04	2.1	203	98	0.00065
7		14.95045	-24.34072	13:46	13:48	4.3	0.15	0.96	0.03	131	1.00	7	0.11	0.886	0.03	236	0.93	57	64.2	35.5	0.27	0.04	0.03	1.8	205	114	0.00047
8		14.95032	-24.34078	13:49	13:51	5.1	0.03	0.78	0.01	167	0.99	12	0.24	0.949	0.04	116	0.61	80	40.8	58.7	0.35	0.01	0.08	0.7	113	163	0.00206
9		14.95044	-24.34065	13:52	13:55	6.9	0.05	0.64	0.02	108	0.99	7	0.14	0.932	0.02	192	0.82	54	63.7	35.9	0.33	0.02	0.05	1.8	183	103	0.00073
10		14.95061	-24.34068	13:57	14:00	35.2	0.79	0.85	0.21	207	0.98	18	0.15	0.82	0.04	404	0.92	74	65.9	33.7	0.16	0.13	0.02	2.0	226	115	0.00037
11		14.95066	-24.34072	14:00	14:04	6.5	0.23	0.82	0.06	149	0.98	12	0.13	0.885	0.03	374	0.96	44	71.4	28.3	0.19	0.04	0.02	2.5	304	121	0.00035
12		14.95067	-24.34085	14:04	14:11	1.4	0.2	0.86	0.03	176	0.98	9	0.16	0.395	0.08	356	0.87	56	66.7	33.1	0.19	0.04	0.03	2.0	296	147	0.00045
13		14.95073	-24.34088	14:11	14:15	5.8	0.22	0.91	0.04	148	0.99	8	0.15	0.84	0.04	390	0.94	57	72.3	27.4	0.19	0.04	0.03	2.6	319	121	0.00038
14	316	14.95064	-24.34064	14:17	14:18	24.7	0.85	0.33	1.42	172	0.70	134	0.05	0.144	0.14	311	0.62	283	64.1	35.5	0.21	0.18	0.01	1.8	168	93	0.00016
15	315	14.95064	-24.34065	14:18	14:20	61.5	1.48	0.71	0.88	240	0.95	54	0.2	0.884	0.07 *(0.09-0.1)£*	482	0.97	73	66.5	33.2	0.14	0.20	0.03	2.0	194	97 *(94-107)£*	0.00042
16		14.95062	-24.34061	14:21	14:25	14.2	0.45	0.83	0.11	160	0.98	13	0.14	0.916	0.02	442	0.89	81	73.2	26.6	0.17	0.07	0.02	2.8	305	111	0.00032
17		14.95071	-24.34055	14:26	14:32	9.1	0.28	0.89	0.04	154	0.99	7	0.17	0.915	0.02	362	0.92	44	69.9	29.8	0.19	0.05	0.03	2.3	283	120	0.00047
MEAN*							**0.3**			**153**			**0.2**			**299**			**64.1**	**35.6**	**0.2**	**0.06**	**0.04**	**1.9**	**225**	**118**	**0.00064**
1 SD*							**0.4**			**33**			**0.04**			**109**			**9.2**	**9.1**	**0.08**	**0.06**	**0.02**	**0.6**	**67**	**18**	**0.00049**
BULK		14.95073	-24.34196	11:37	12:01	0.15	0.12	0.70	0.04	-	-	-	-	-	-	-	-	-	-	-	-	-	-	-	-	-	-

Table 2 - Chemistry (in mol %) of major and minor dry gas components in Pico do Fogo F15 fumarole. H_2/H_2S and CO_2/H_2S ratios are reported for comparison with the same ratios calculated by Multi-GAS

Sample	T °C	date	He ppm	H_2 ppm	O_2 %	N_2 %	CH_4 ppm	CO ppm	CO_2 %	H_2S %	Tot %	H_2/H_2S	CO_2/H_2S
F15a	315	05/02/2019	8	952	0.11	0.51	0.7	15	97.03	1.03	98.8	0.09	94.20
F15b			8	979	0.33	1.4	1.3	17	95.83	0.96	98.6	0.10	99.82
F15c			6	373	12.63	46.35	2.1	13	39.6	0.37	99.0	0.10	107.03

Table 3 - Volatile fluxes from Fogo island. All data in tons/day

	Summit Fumarolic Field*		Diffuse Degassing°		Eruptive degassing (2014 eruption)[£]	Eruptive degassing (time integrated)[$]
	Mean	1 SD	Mean	1 SD	Mean	Mean
SO_2 flux	1.4	0.4	-	-	10118	82
H_2O flux	780	320	330	-	24245	196
CO_2 flux	1060	340	147-219 (828[@])	35-36	10668	86
H_2S flux	6.2	2.4	0.025	0.007	57	0.5
H_2 flux	0.05	0.022	0.033	0.0105	0.2	0.002

*This work; °inner crater floor; Dionis et al., 2014; [@]whole island; Dionis et al., 2015; [£]Measured on November 30, 2014; Hernández et al., 2015; [$]This study, recalculated from data in Hernández et al., 2015

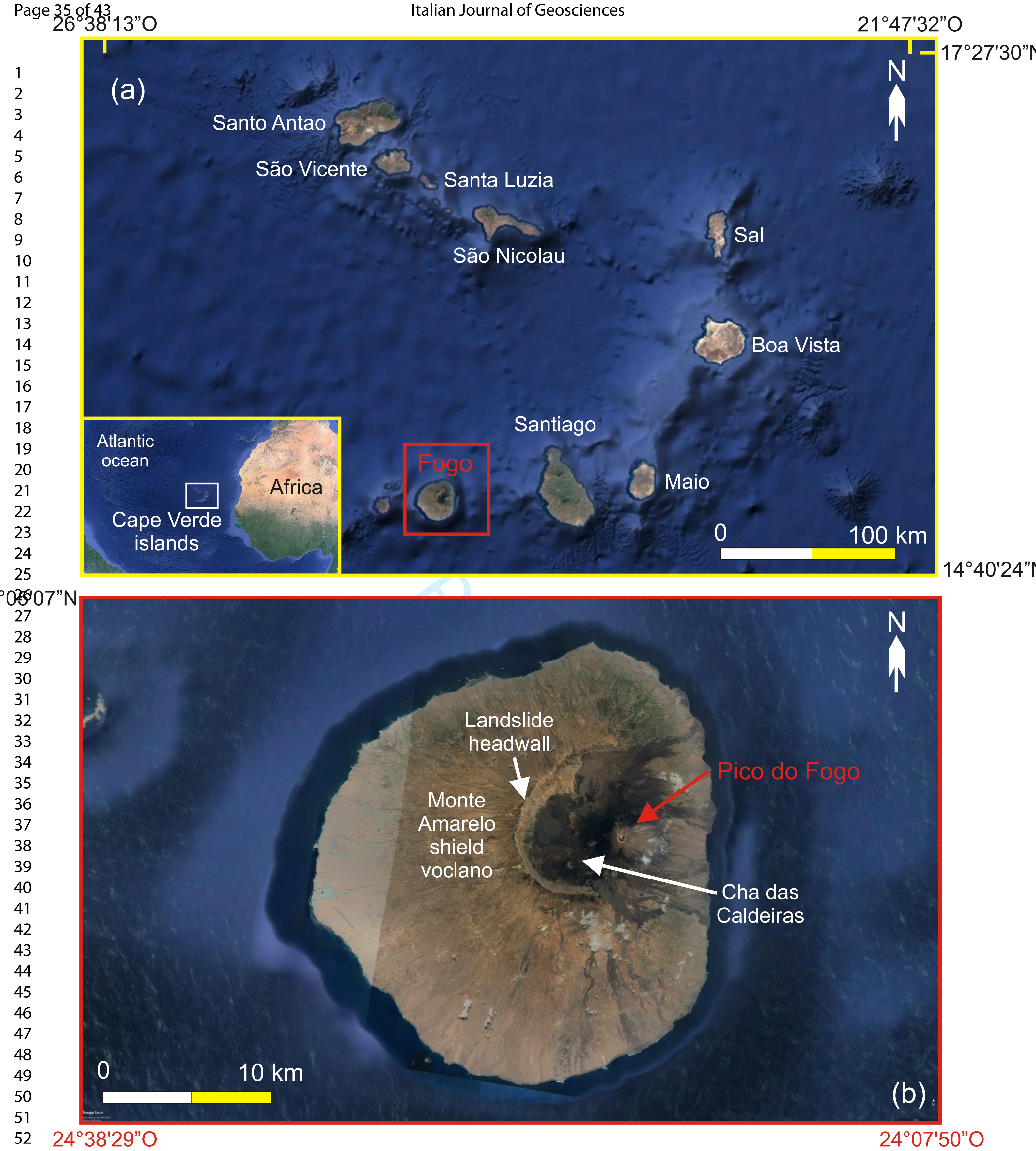
26°38'13"O
21°47'32"O
17°27'30"N
(a)
N
Santo Antao
São Vicente
Santa Luzia
São Nicolau
Sal
Boa Vista
Santiago
Fogo
Maio
0
100 km
14°40'24"N
Atlantic ocean
Africa
Cape Verde islands
°05'07"N
N
Landslide headwall
Pico do Fogo
Monte Amarelo shield voclano
Cha das Caldeiras
0
10 km
(b)
24°38'29"O
24°07'50"O

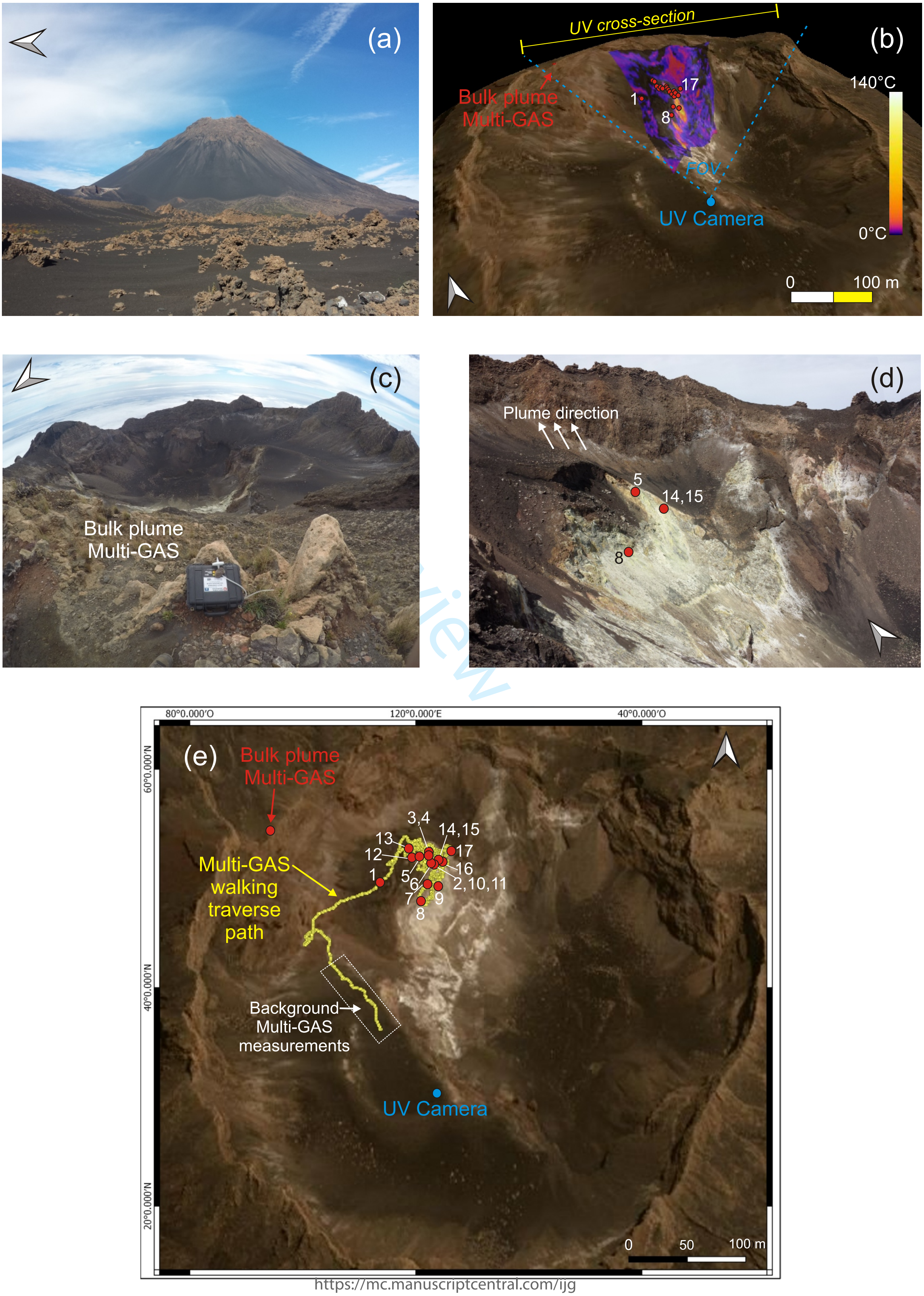
(a)
(b)
UV cross-section
Bulk plume
Multi-GAS
17
1
8
FOV
UV Camera
140°C
0°C
0
100 m
(c)
Bulk plume
Multi-GAS
(d)
Plume direction
5
14,15
8
80°0.000'O
120°0.000'E
40°0.000'O
60°0.000'N
40°0.000'N
20°0.000'N
(e)
Bulk plume
Multi-GAS
Multi-GAS
walking
traverse
path
3,4
13
14,15
12
17
1
5
16
6
2,10,11
7
9
8
Background
Multi-GAS
measurements
UV Camera
0
50
100 m

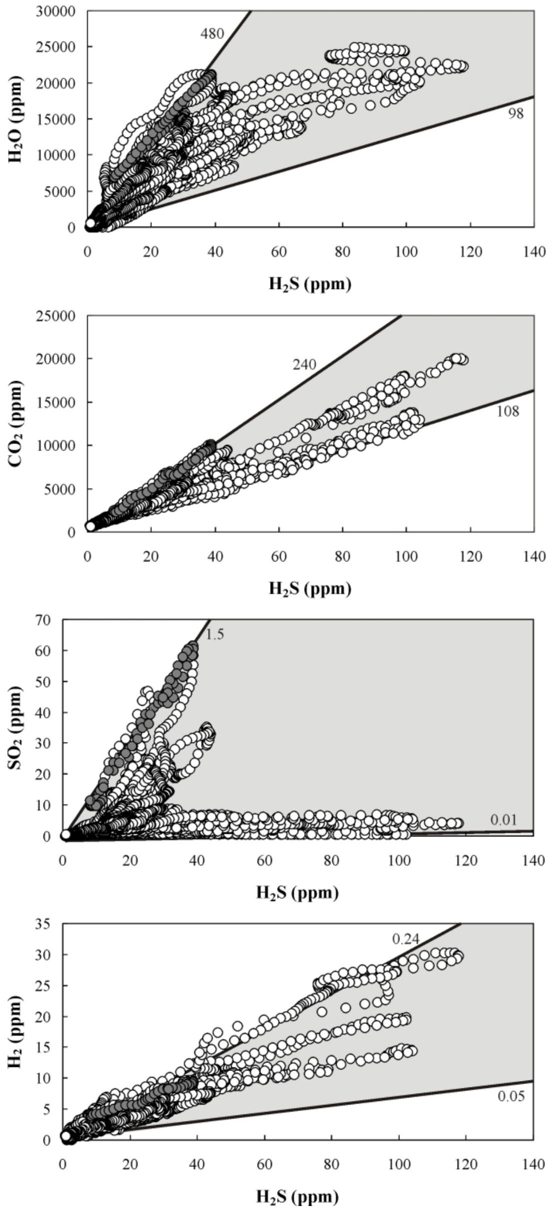

143x319mm (300 x 300 DPI)

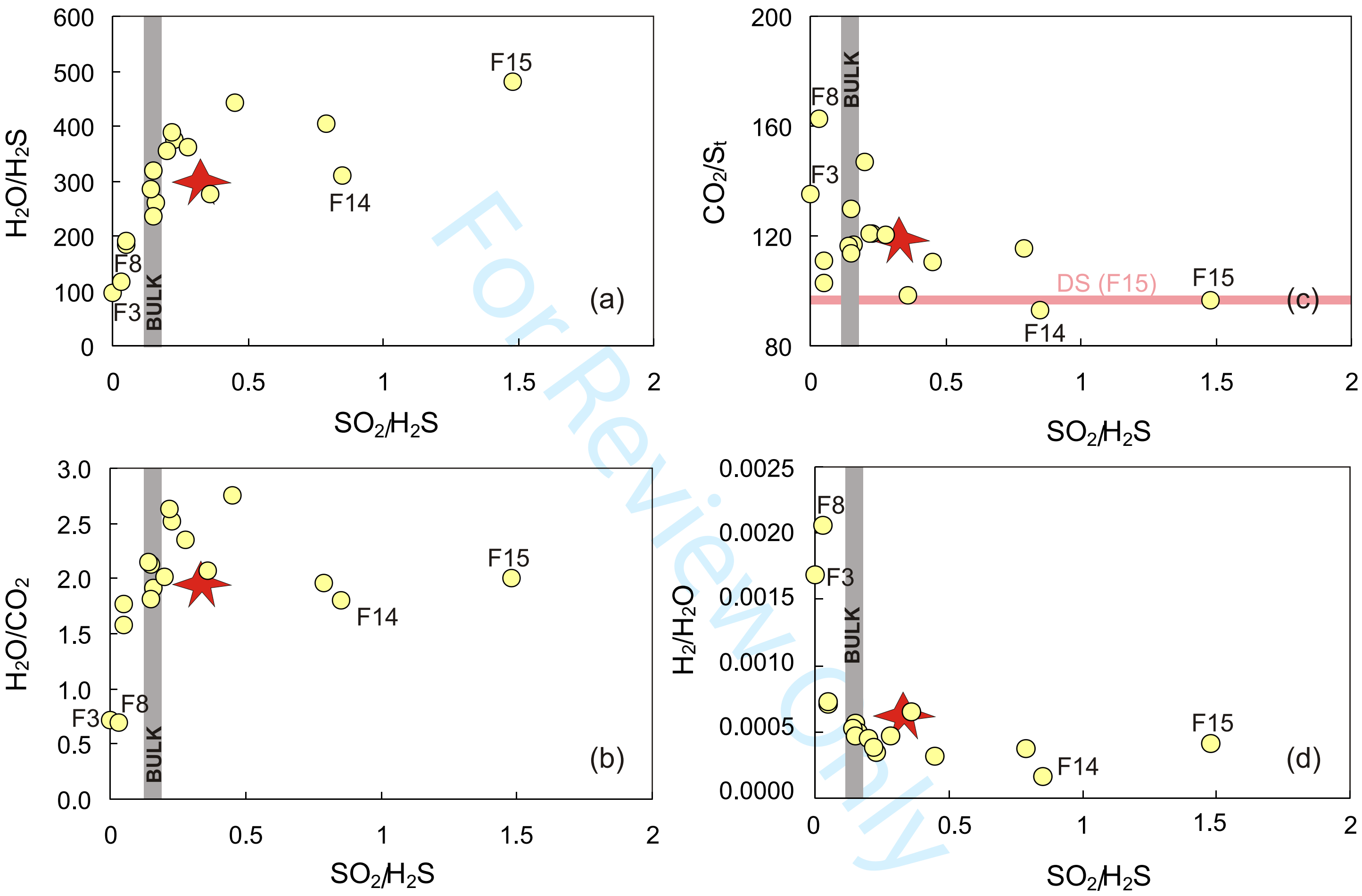
(a)
H_2O/H_2S
600
500
400
300
200
100
0
F15
F14
F8
F3
BULK
0
0.5
1
1.5
2
SO_2/H_2S
(c)
CO_2/S_t
200
160
120
80
F8
F3
BULK
DS (F15)
F15
F14
0
0.5
1
1.5
2
SO_2/H_2S
(b)
H_2O/CO_2
3.0
2.5
2.0
1.5
1.0
0.5
0.0
F15
F14
F8
F3
BULK
0
0.5
1
1.5
2
SO_2/H_2S
(d)
H_2/H_2O
0.0025
0.0020
0.0015
0.0010
0.0005
0.0000
F8
F3
BULK
F15
F14
0
0.5
1
1.5
2
SO_2/H_2S

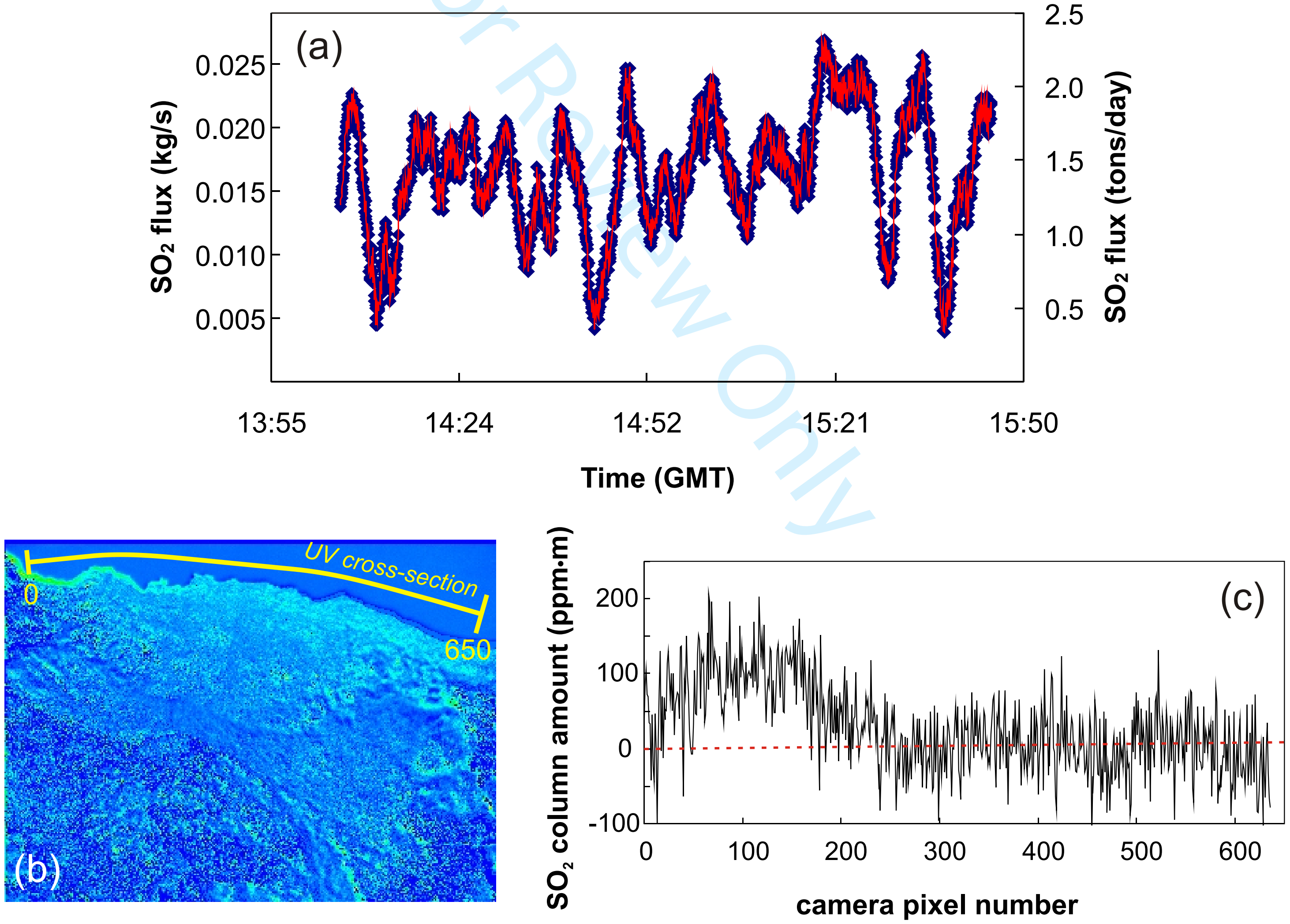
(a)
0.025
0.020
0.015
0.010
0.005
SO_2 flux (kg/s)
2.5
2.0
1.5
1.0
0.5
SO_2 flux (tons/day)
13:55
14:24
14:52
15:21
15:50
Time (GMT)
UV cross-section
0
650
(b)
(c)
200
100
0
-100
SO_2 column amount (ppm·m)
0
100
200
300
400
500
600
camera pixel number

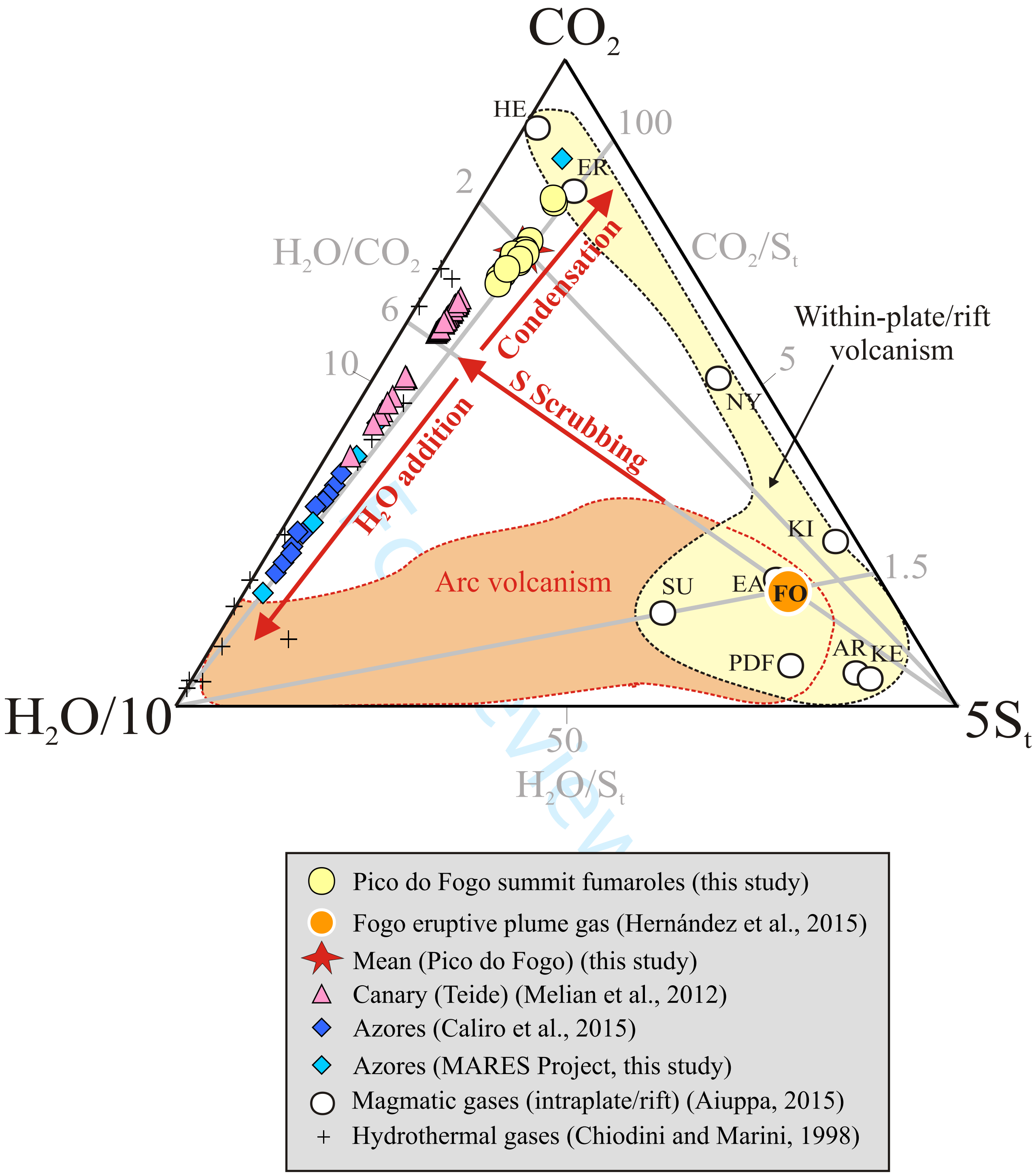
CO_2
$H_2O/10$
$5S_t$
100
2
6
10
5
1.5
50
H_2O/CO_2
CO_2/S_t
H_2O/S_t
HE
ER
NY
KI
SU
EA
FO
PDF
AR
KE
Condensation
S Scrubbing
H_2O addition
Arc volcanism
Within-plate/rift volcanism
○ Pico do Fogo summit fumaroles (this study)
● Fogo eruptive plume gas (Hernández et al., 2015)
★ Mean (Pico do Fogo) (this study)
△ Canary (Teide) (Melian et al., 2012)
◆ Azores (Caliro et al., 2015)
◆ Azores (MARES Project, this study)
○ Magmatic gases (intraplate/rift) (Aiuppa, 2015)
+ Hydrothermal gases (Chiodini and Marini, 1998)

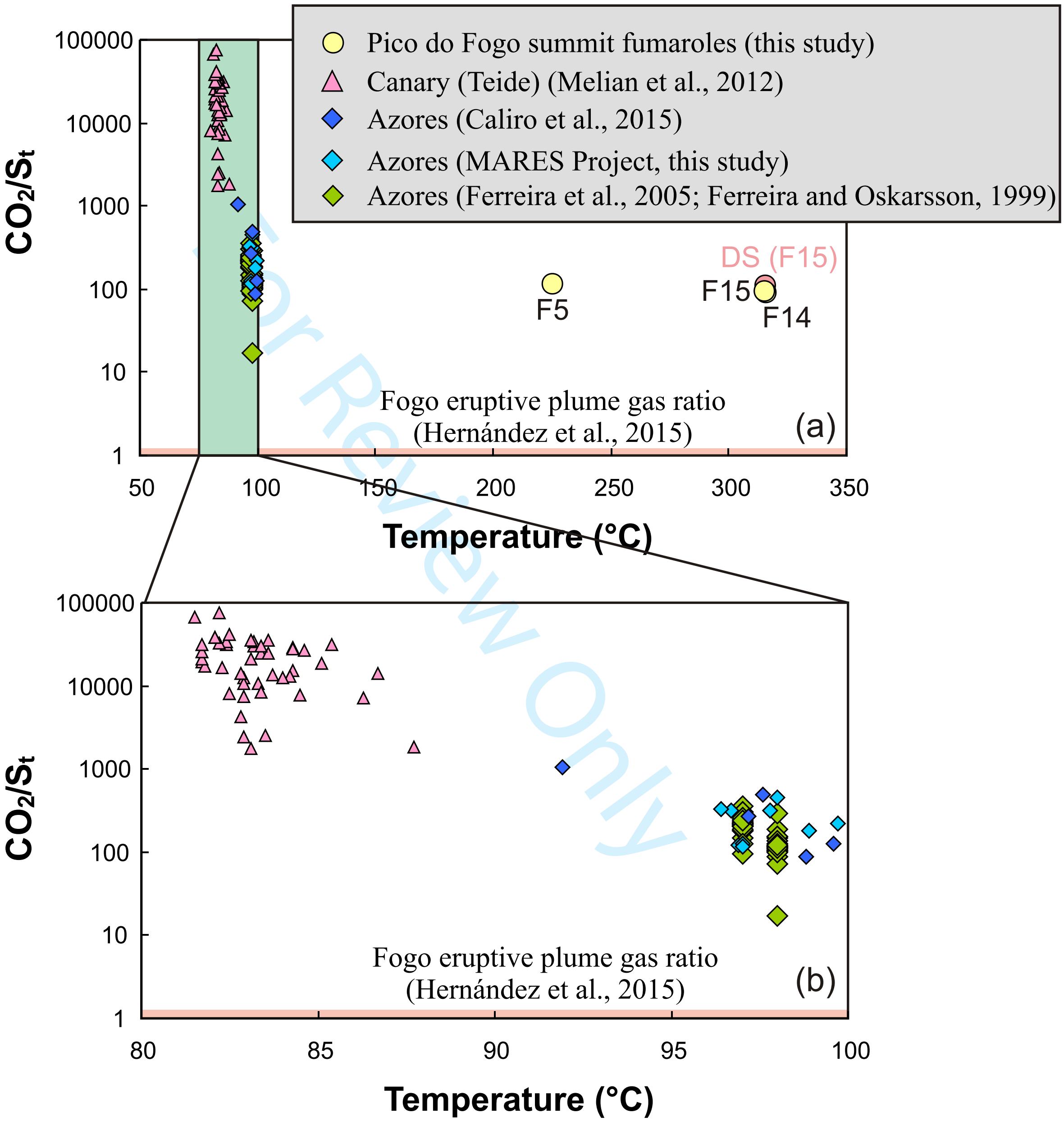
Pico do Fogo summit fumaroles (this study)
Canary (Teide) (Melian et al., 2012)
Azores (Caliro et al., 2015)
Azores (MARES Project, this study)
Azores (Ferreira et al., 2005; Ferreira and Oskarsson, 1999)
CO_2/S_t
100000
10000
1000
100
10
1
DS (F15)
F5
F15
F14
Fogo eruptive plume gas ratio
(Hernández et al., 2015)
(a)
50
100
150
200
250
300
350
Temperature (°C)
CO_2/S_t
100000
10000
1000
100
10
1
Fogo eruptive plume gas ratio
(Hernández et al., 2015)
(b)
80
85
90
95
100
Temperature (°C)

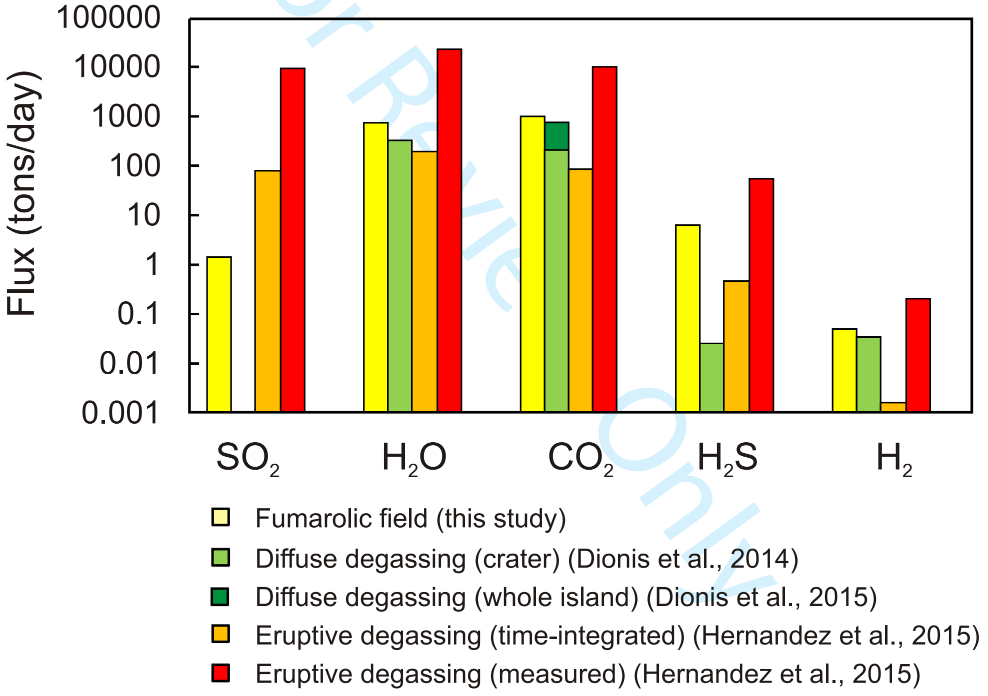
Flux (tons/day)
100000
10000
1000
100
10
1
0.1
0.01
0.001
SO_2
H_2O
CO_2
H_2S
H_2
Fumarolic field (this study)
Diffuse degassing (crater) (Dionis et al., 2014)
Diffuse degassing (whole island) (Dionis et al., 2015)
Eruptive degassing (time-integrated) (Hernandez et al., 2015)
Eruptive degassing (measured) (Hernandez et al., 2015)

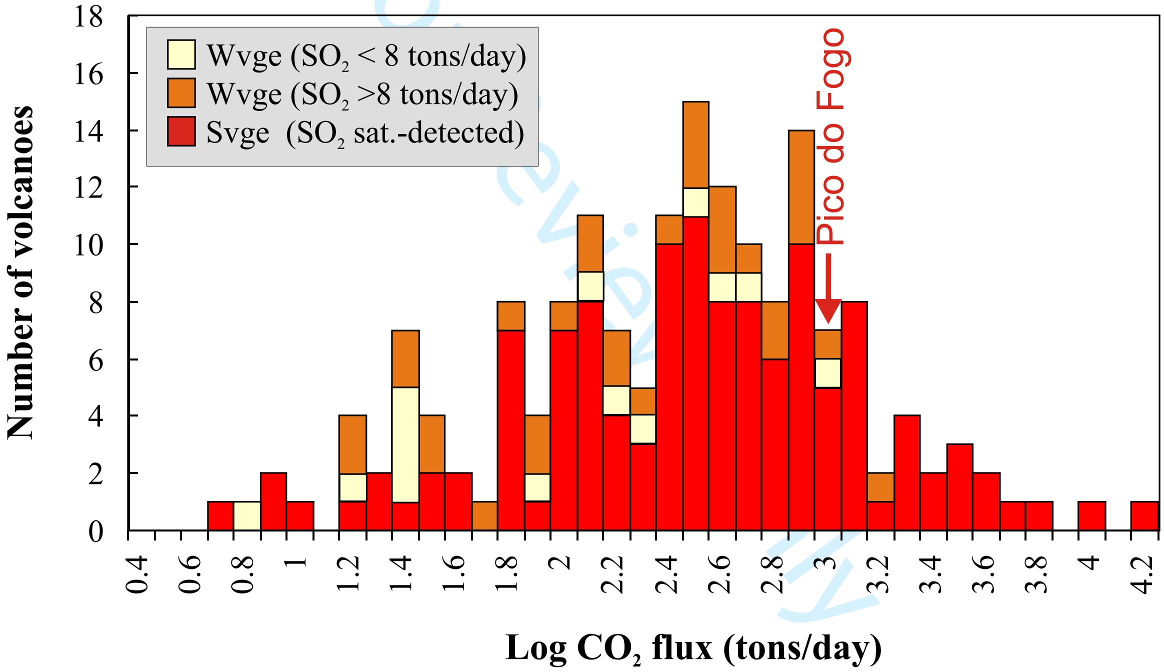
Wvge (SO2 < 8 tons/day)
Wvge (SO2 >8 tons/day)
Svge (SO2 sat.-detected)
Pico do Fogo
Number of volcanoes
Log CO2 flux (tons/day)
0
2
4
6
8
10
12
14
16
18
0.4
0.6
0.8
1
1.2
1.4
1.6
1.8
2
2.2
2.4
2.6
2.8
3
3.2
3.4
3.6
3.8
4
4.2